

2015 Fall

“Phase Transformation *in* Materials”

11.18.2015

Eun Soo Park

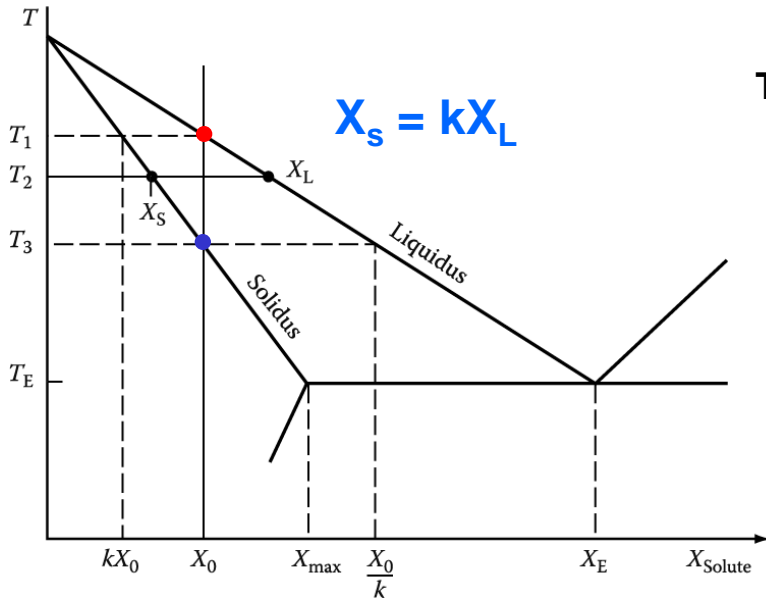
Office: 33-313

Telephone: 880-7221

Email: espark@snu.ac.kr

Office hours: by an appointment

1) Equilibrium Solidification : perfect mixing in solid and liquid

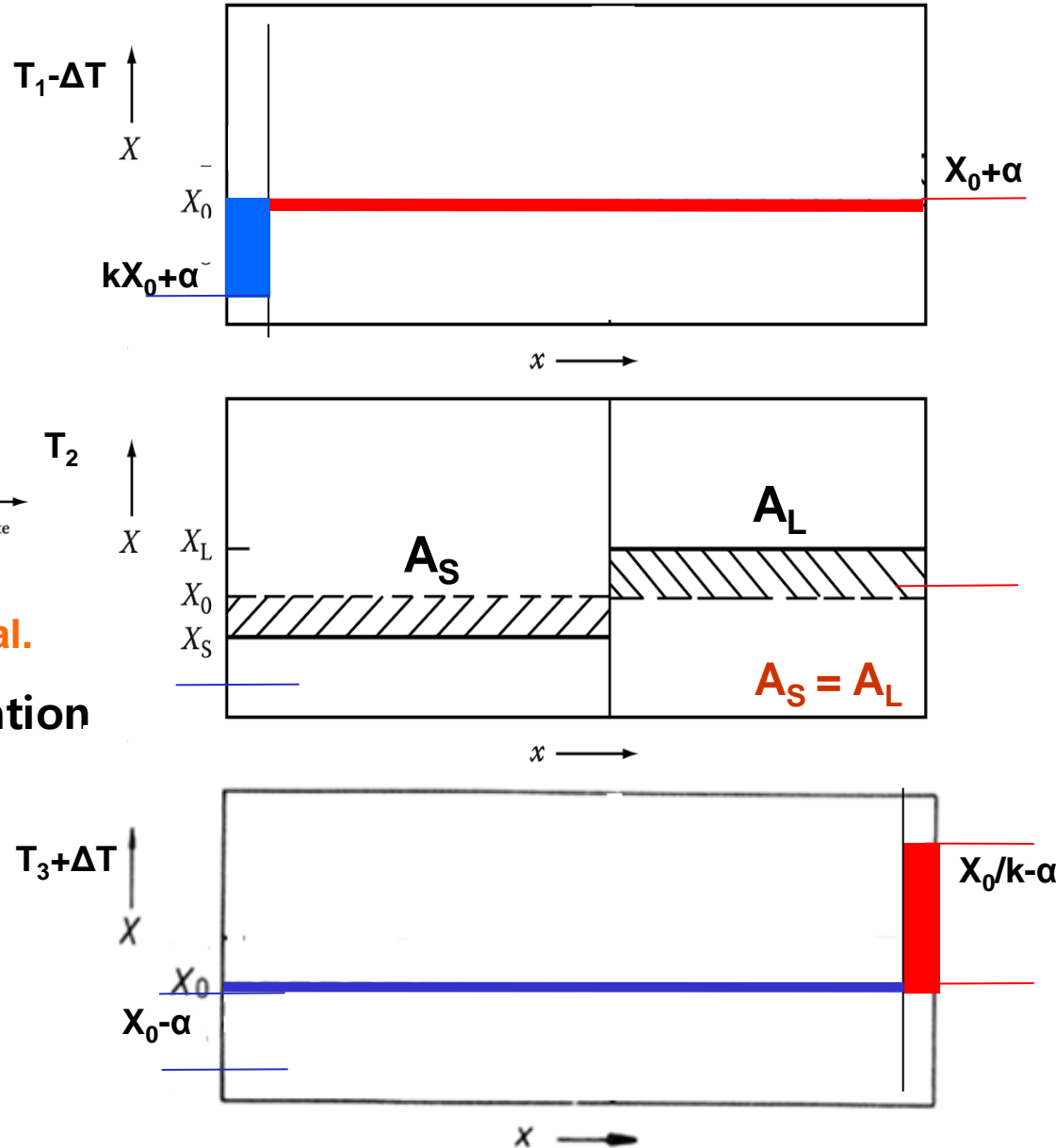
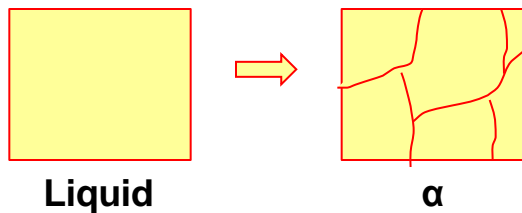


Conservation of solute requires the two shaded areas to be equal.

* Equilibrium solute concentration

$$kX_0 \leq X_s \leq X_0$$

$$X_0 \leq X_L \leq X_0/k < X_E$$



2) Non-equilibrium Solidification: No Diffusion in Solid, Perfect Mixing in Liquid

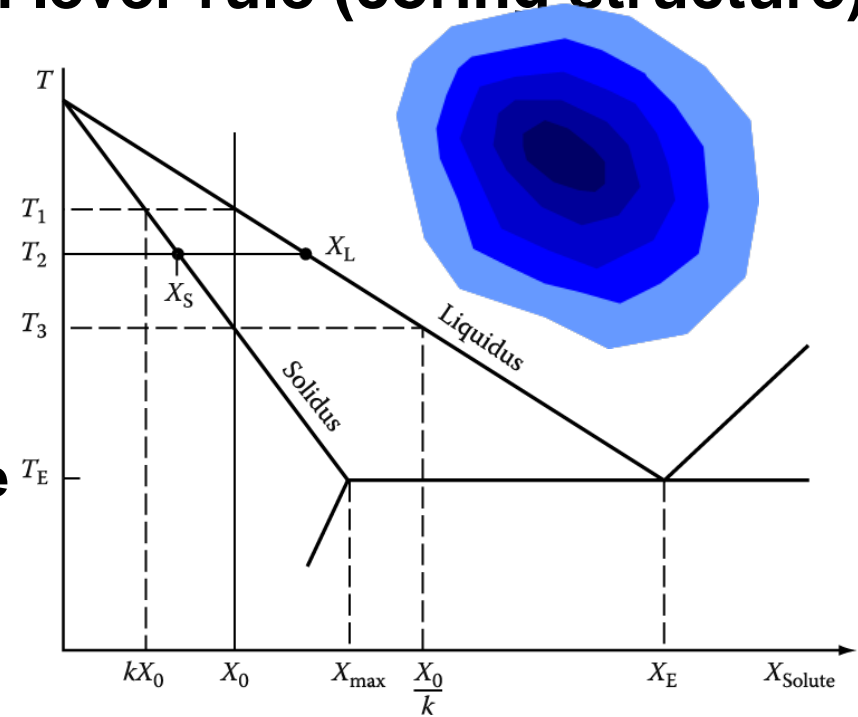
Mass balance: non-equilibrium lever rule (coring structure)

When cooled by dT from any arbitrary T , determine the followings.

: solute ejected into the liquid = ?
 → solute increase in the liquid

Ignore the difference in molar volume between the solid and liquid.

f_s : volume fraction solidified



solute ejected into the liquid=?

→ proportional to what?

$$df_s \quad (X_L - X_S)$$

solute increase in the liquid=?

→ proportional to what?

$$(1-f_s) \quad dX_L$$

$$(X_L - X_S)df_s = (1-f_s)dX_L$$

Solve this equation.

when $f_s = 0 \rightarrow X_S, X_L$?

$$X_S = kX_0 \text{ and } X_L = X_0$$

Initial conditions

$$\int_0^{f_S} \frac{df_S}{1-f_S} = \int_{X_0}^{X_L} \frac{dX_L}{X_L - X_S} = \int_{X_0}^{X_L} \frac{dX_L}{X_L - kX_L} = \int_{X_0}^{X_L} \frac{dX_L}{X_L(1-k)}$$

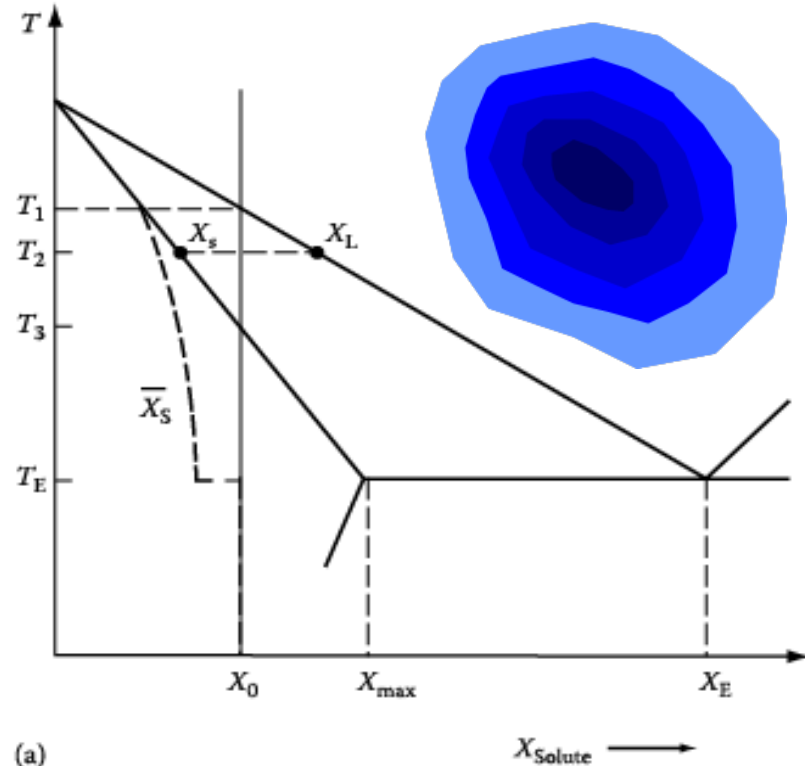
$$\int_0^{f_S} (1-k)(-1)d \ln(1-f_S) = \int_{X_0}^{X_L} d \ln X_L$$

$$\ln \frac{X_L}{X_0} = (k-1) \ln(1-f_S)$$

$$\therefore X_L = X_0 f_L^{(k-1)} \quad X_S = kX_L$$

$$X_S = kX_0 (1-f_S)^{(k-1)}$$

**: non-equilibrium lever rule
(Scheil equation)**



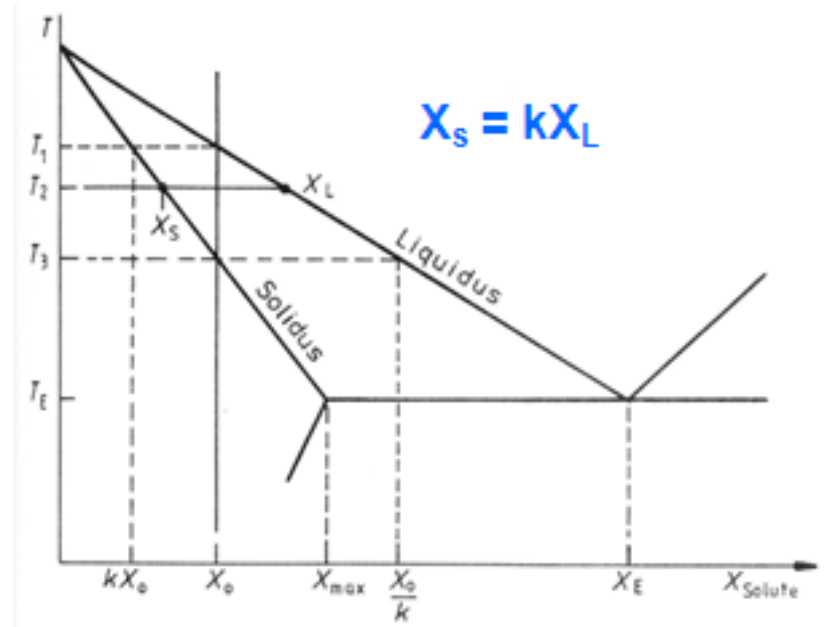
→ quite generally applicable even for nonplanar solid/liquid interfaces provided here, the liquid composition is uniform and that the Gibbs-Thomson effect is negligible.

“If $k < 1$: predicts that if no diff. in solid, some eutectic always exist to solidify.”
($X_S < X_L$)

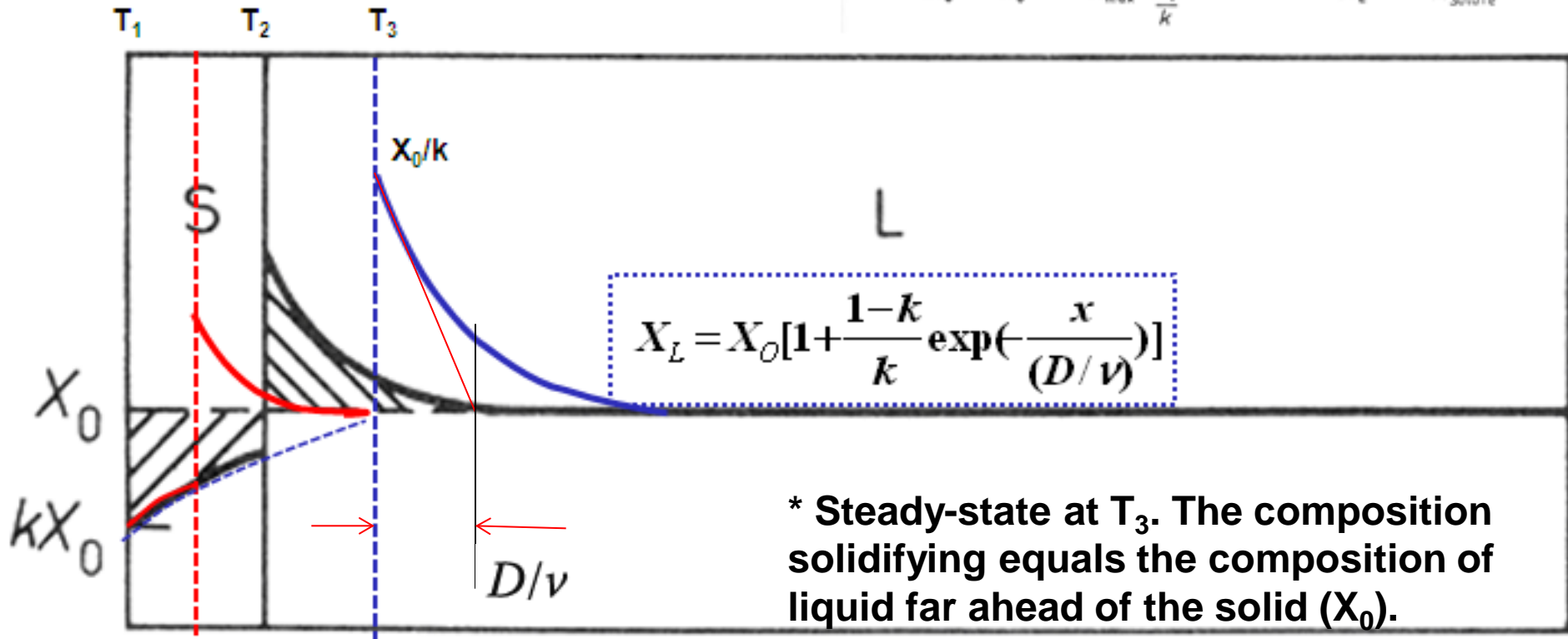
“Alloy solidification”

- Solidification of single-phase alloys

* No Diffusion on Solid,
Diffusional Mixing in the Liquid



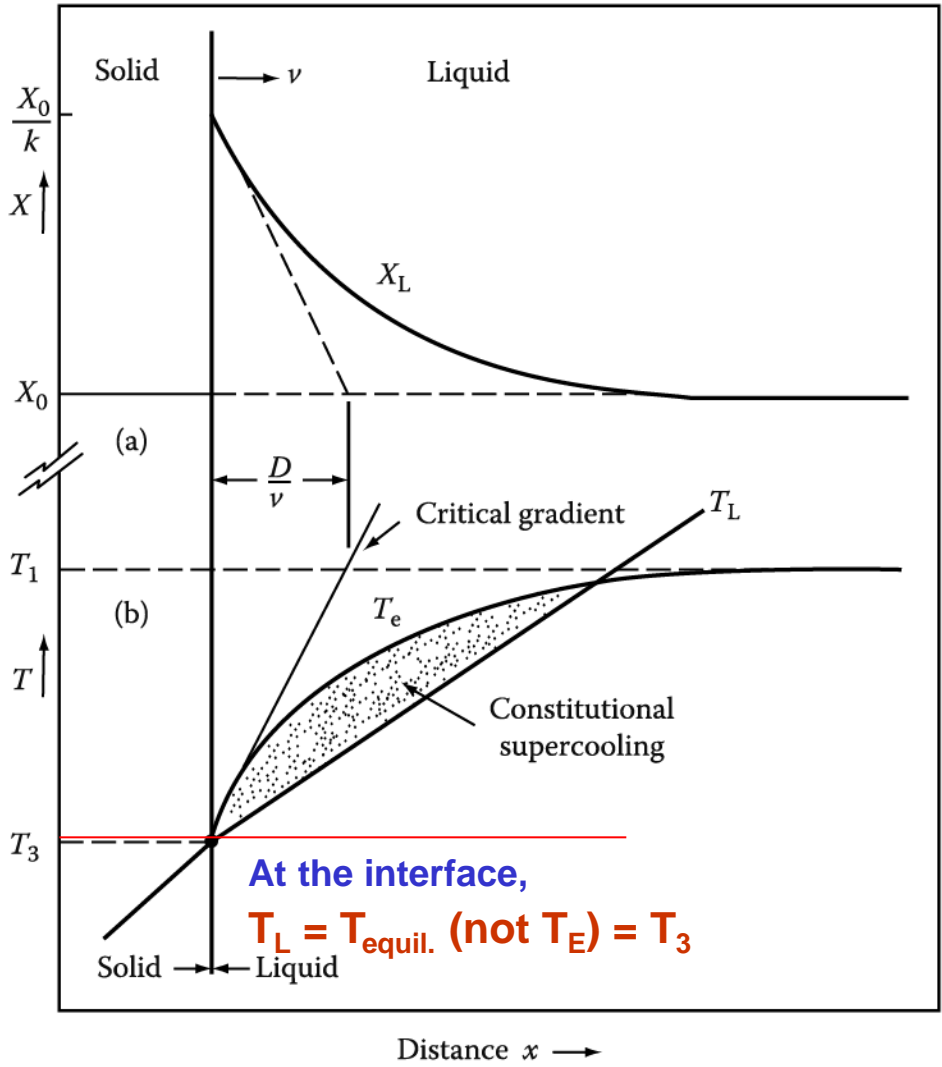
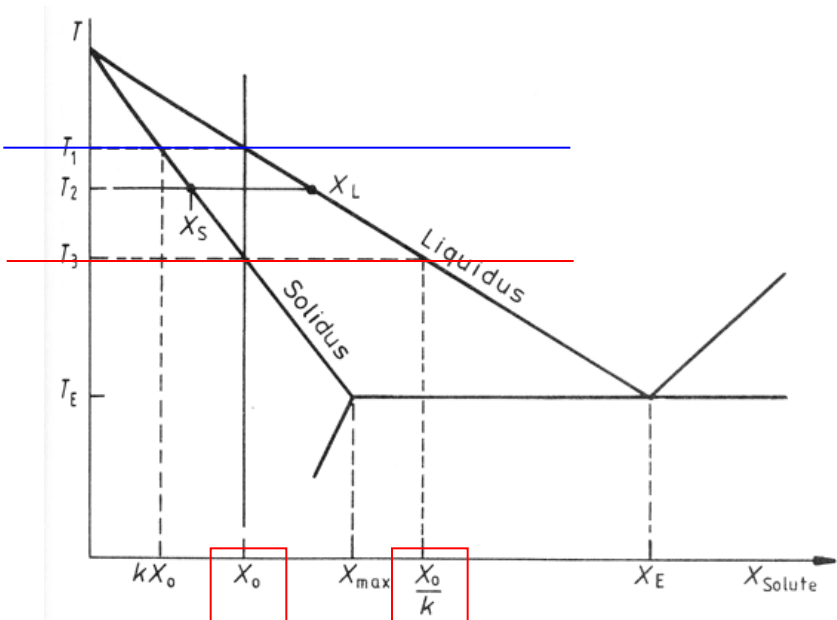
Interface temperature



* Steady-state at T_3 . The composition solidifying equals the composition of liquid far ahead of the solid (X_0).

* Constitutional Supercooling

No Diffusion on Solid, Diffusional Mixing in the Liquid → **Steady State**



* Actual temperature gradient in Liquid

$$T_L'$$

* equilibrium solidification temp. change

$$T_{\text{equil.}}$$

At the interface,
 $T_L = T_{\text{equil. (not } T_E)} = T_3$

$T_L' > (T_1 - T_3)/(D/v)$: the protrusion melts back → **Planar interface: stable**

$T_L' / v < (T_1 - T_3)/D$: **Constitutional supercooling** → **cellular/ dendritic growth**

Cellular Solidification: formation by constitutional supercooling in superheated liquid

If temperature gradient ahead of an initially planar interface is gradually reduced below the critical value, (constitutional supercooling at solid/liquid interface)

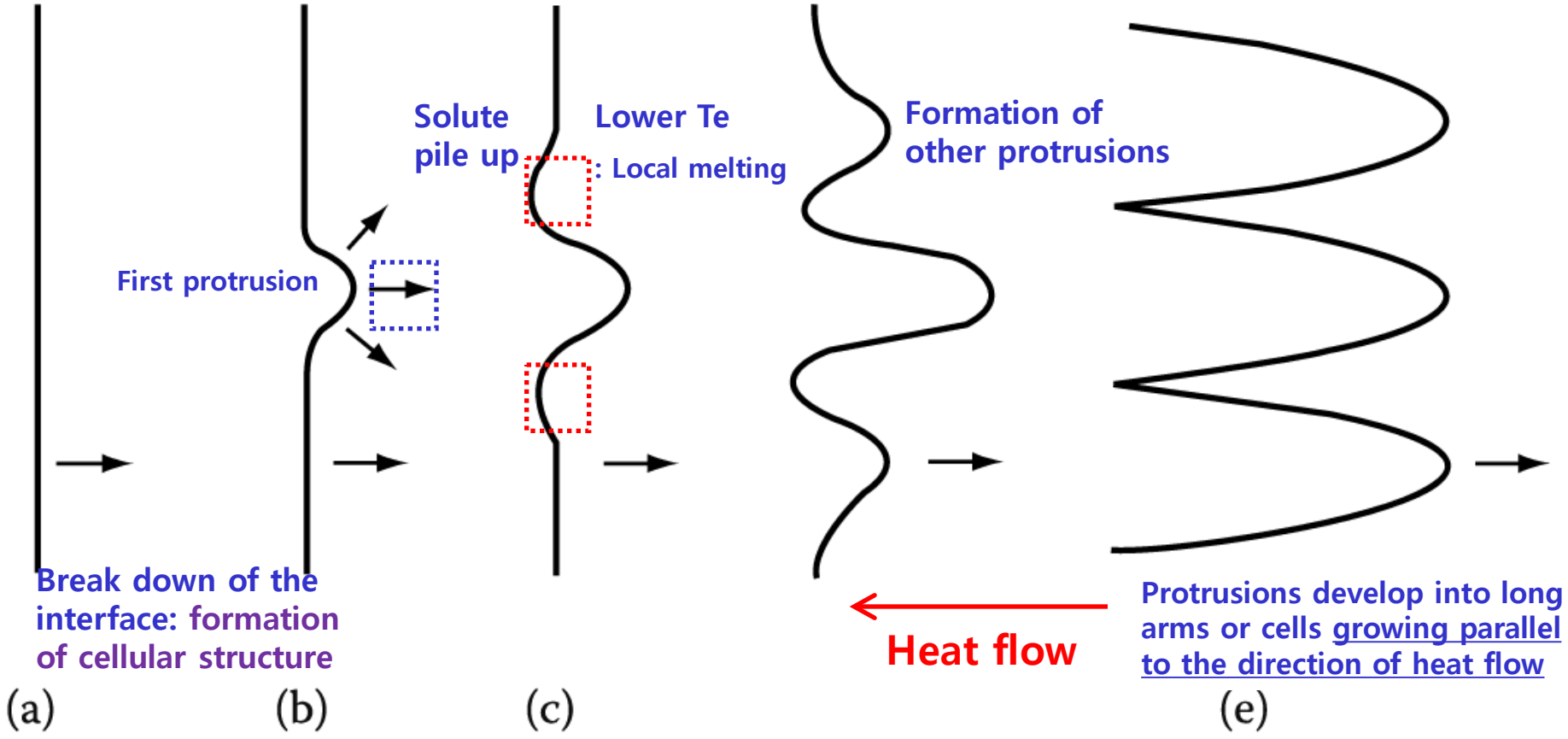


Fig. 4.24 The breakdown of an initially planar solidification front into cells

Solidification of Pure Metal

: Thermal gradient dominant



Solidification of single phase alloy: Solute redistribution dominant

a) Constitutional supercooling

Planar → Cellular growth → cellular dendritic growth → Free dendritic growth

응고계면에 조성적 과냉의
thin zone 형성에 의함
Dome 형태 선단 / 주변에
hexagonal array

$T \downarrow \rightarrow$ 조성적 과냉영역 증가
Cell 선단의 피라미드형상/ 가지
들의 square array/ Dendrite
성장방향쪽으로 성장방향 변화

성장하는 crystal로 부터 발생한
잠열을 과냉각 액상쪽으로 방출함
에 의해 형성
Dendrite 성장 방향/ Branched
rod-type dendrite

→ “Nucleation of new crystal in liquid”

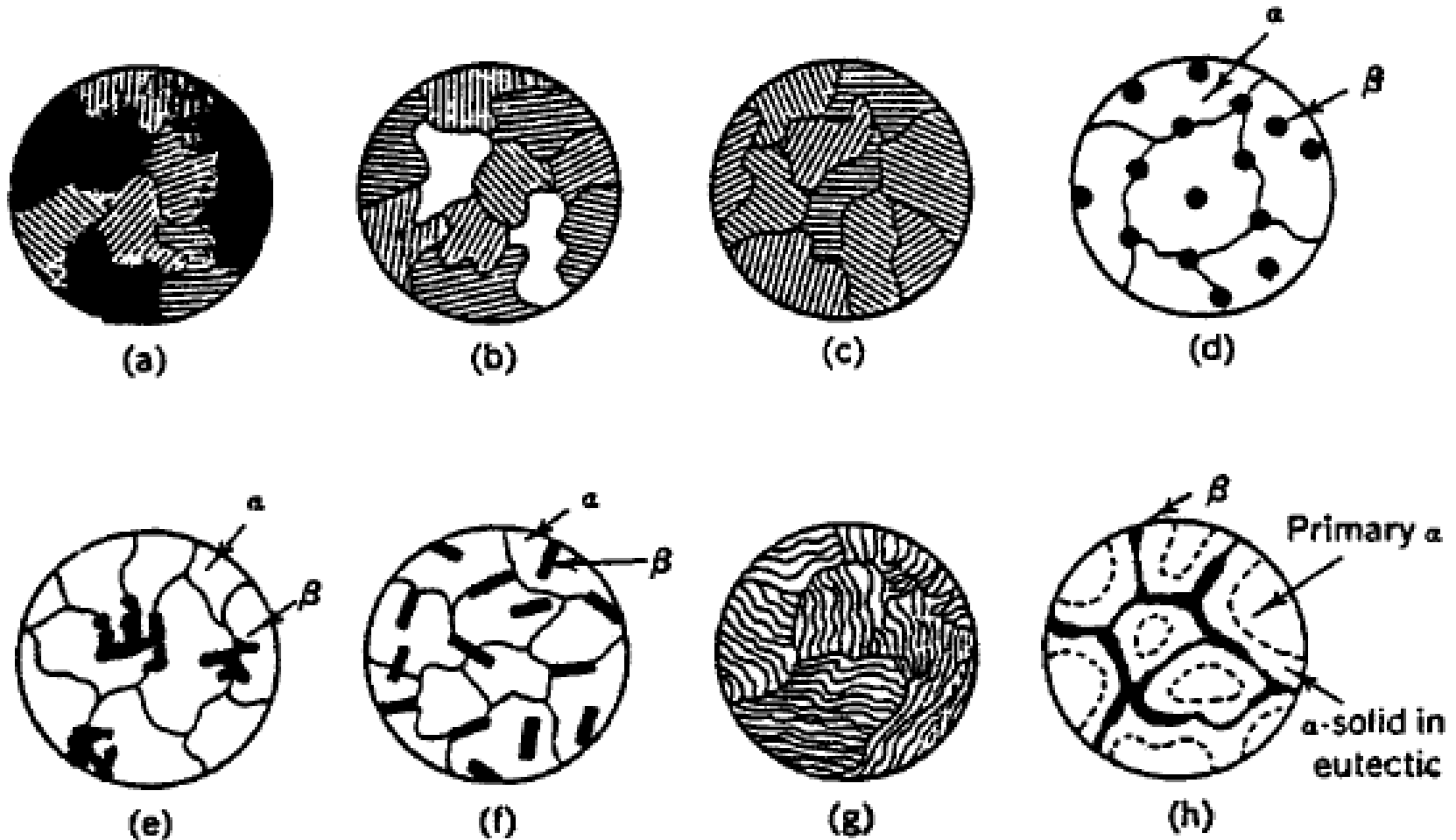
성장이 일어나는 interface 보다 높은 온도

b) Segregation

: normal segregation, grain boundary segregation, cellular segregation, dendritic segregation, inverse segregation, coring and intercrystalline segregation, gravity segregation

Q: Various different types of eutectic solidification ($L \rightarrow \alpha + \beta$) ?

4.3.2 Eutectic Solidification: $L \rightarrow \alpha + \beta$



~~various~~

Fig. 14 Schematic representation possible in eutectic structures. (a), (b) and (c) are alloys shown in fig. 13; (d) nodular; (e) Chinese script; (f) acicular; (g) lamellar; and (h) divorced.

4.3.2 Eutectic Solidification

Various different types of eutectic solidification → Both phases grow simultaneously.

Normal eutectic

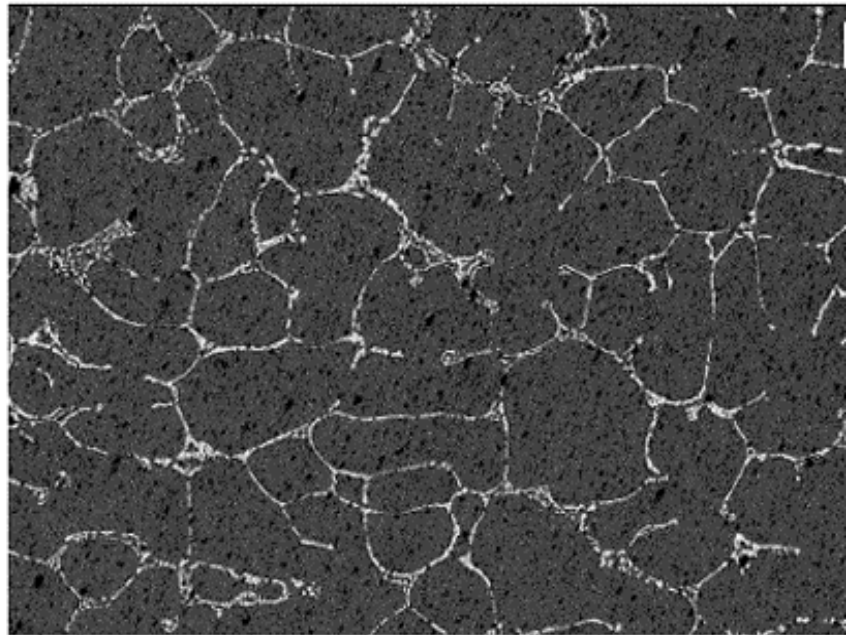
both phases have low entropies of fusion.



Fig. 4.30 Rod-like eutectic. Al_6Fe rods in Al matrix. Transverse section. Transmission electron micrograph (x 70000).

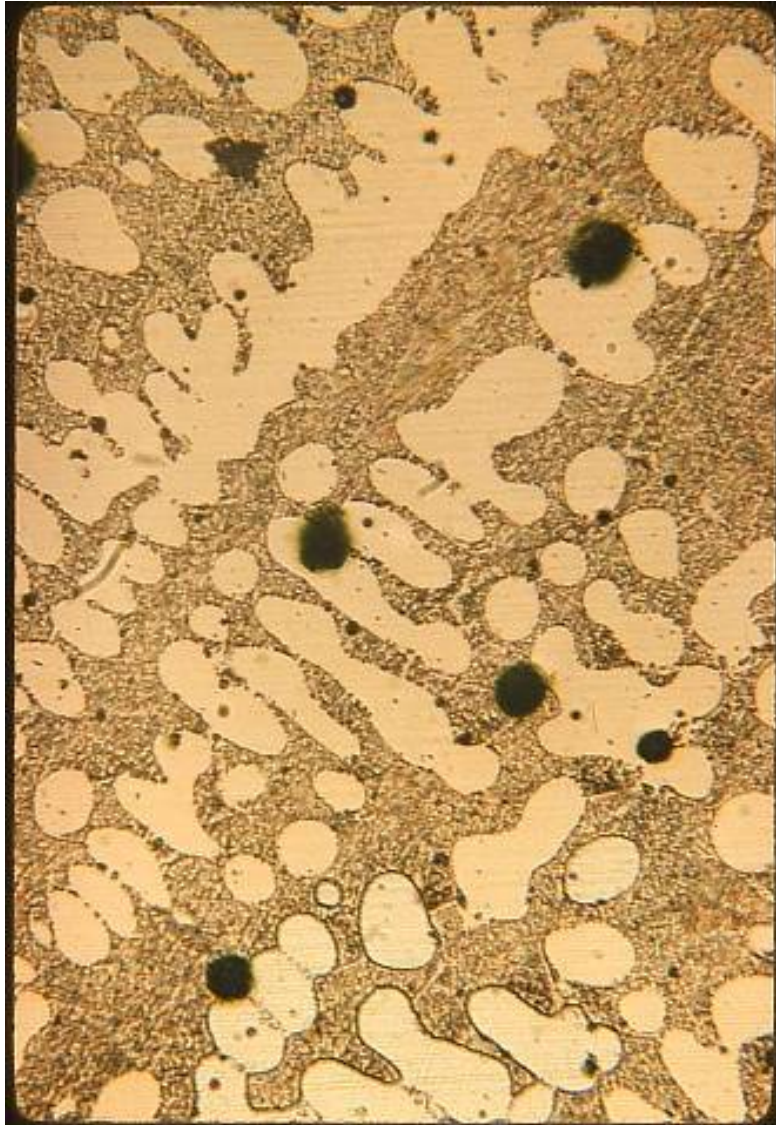
Anomalous eutectic

One of the solid phases is capable of faceting, i.e., has a high entropy of melting.

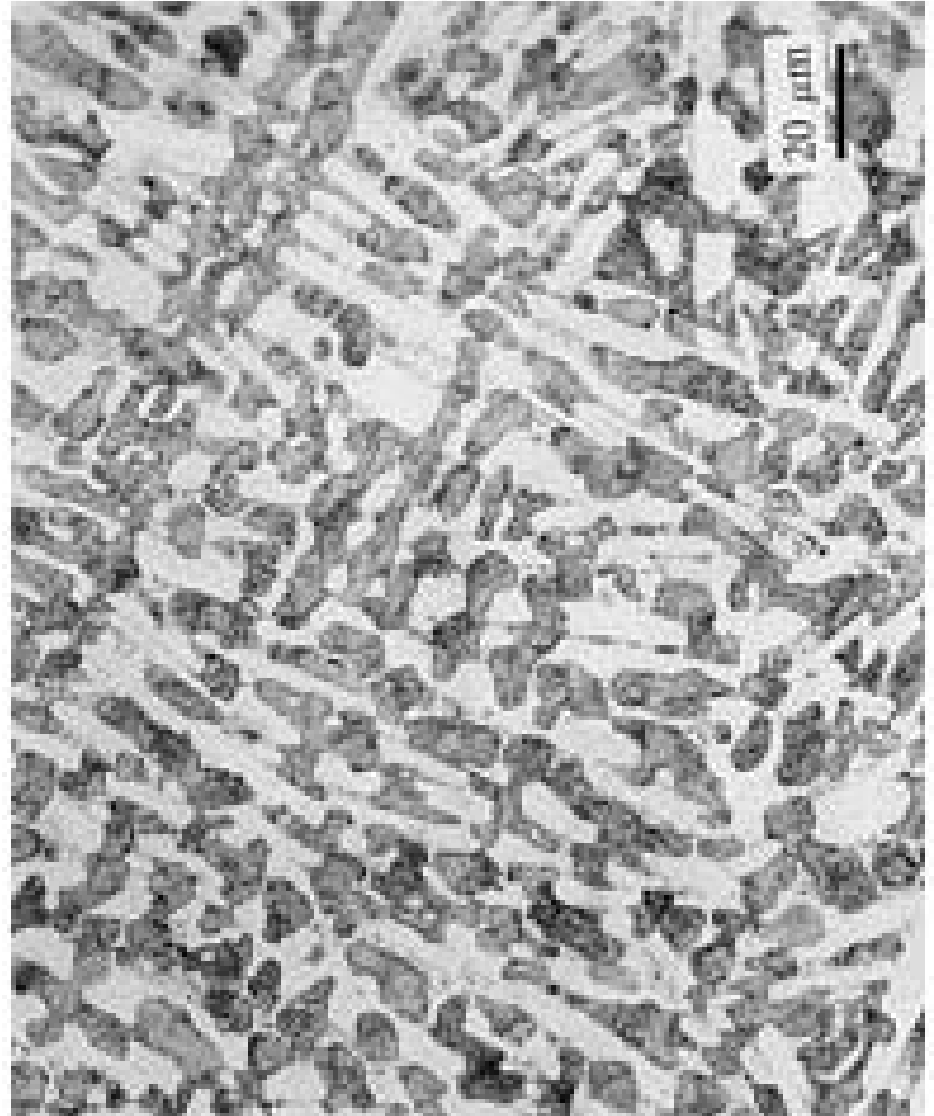


The microstructure of the **Pb-61.9%Sn (eutectic) alloy** presented a coupled growth of the (Pb)/ βSn eutectic. There is a remarkable change in morphology **increasing the degree of undercooling** with transition from regular lamellar to **anomalous eutectic**.

Eutectic



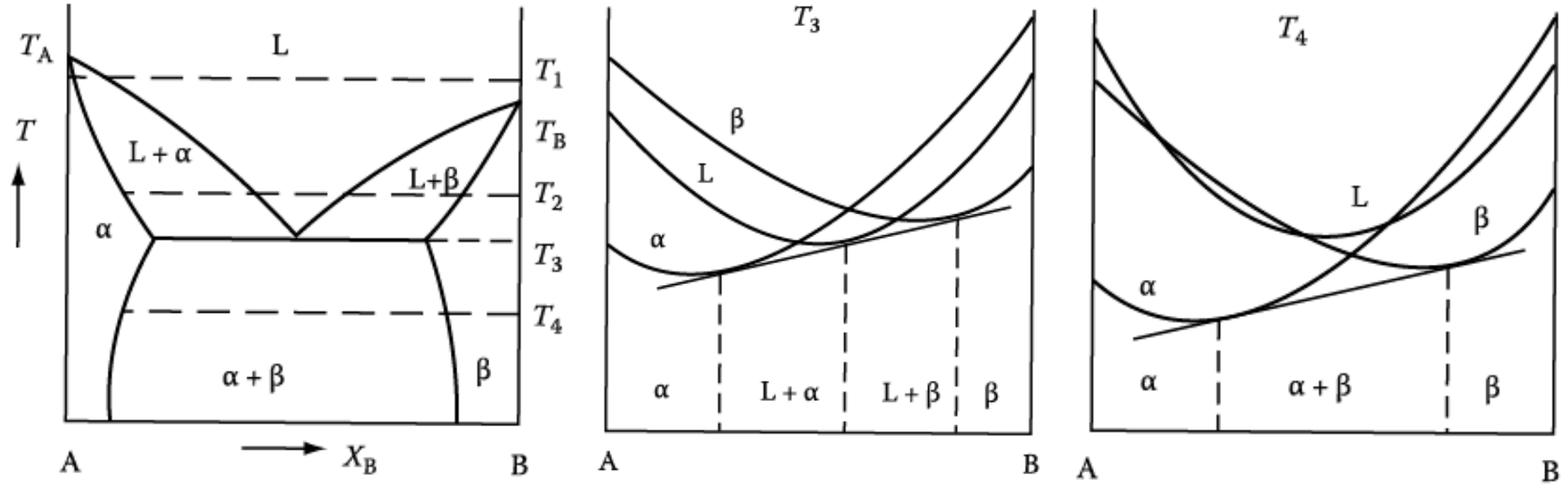
Divorced Eutectic



Q: Thermodynamics and Kinetics of eutectic solidification ($L \rightarrow \alpha + \beta$) ?

This section will only be concerned with normal structures, and deal mainly with lamellar morphologies.

2. Eutectic Solidification (Thermodynamics)



Plot the diagram of Gibbs free energy vs. composition at T_3 and T_4 .

What is the driving force for the eutectic reaction ($L \rightarrow \alpha + \beta$) at T_4 at C_{eut} ?

What is the driving force for nucleation of α and β ? “ ΔT ”

Eutectic Solidification (Kinetics)

: $\Delta T \rightarrow$ formation of interface + solute redistribution

If α is nucleated from liquid and starts to grow, what would be the composition at the interface of α/L determined?

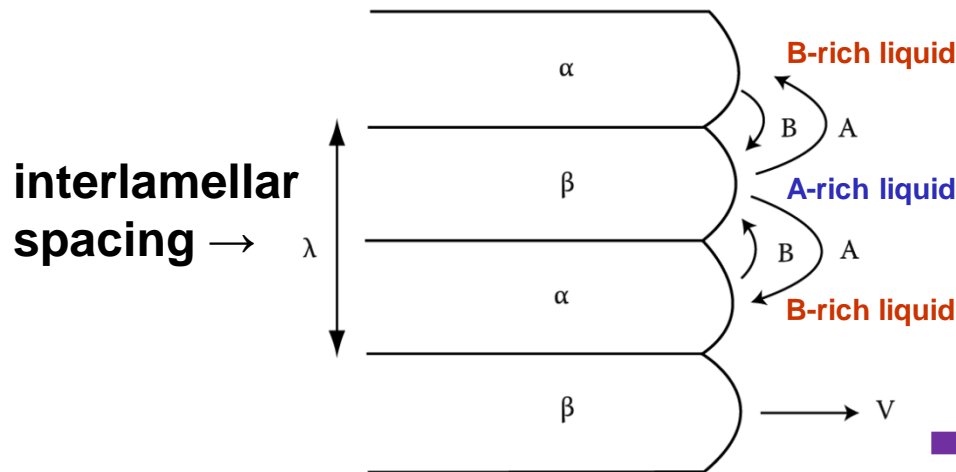
\rightarrow rough interface (diffusion interface) & local equilibrium

How about at β/L ? Nature's choice? Lamellar structure

$$\rightarrow G = G_{\text{bulk}} + G_{\text{interface}} = G_0 + \gamma A$$

$$\sum A_i \gamma_i + \Delta G_S = \text{minimum}$$

Interface energy + Misfit strain energy



Eutectic solidification
: diffusion controlled process

1) $\lambda \downarrow \rightarrow$ eutectic growth rate \uparrow

but 2) $\lambda \downarrow \rightarrow \alpha/\beta$ interfacial $E, \gamma_{\alpha\beta} \uparrow$
 \rightarrow lower limit of λ

\rightarrow fastest growth rate at a certain λ

What would be a role of the curvature at the tip?

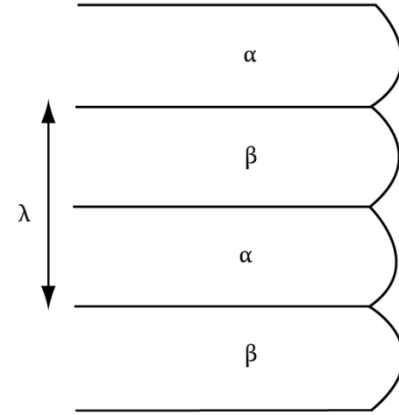
\rightarrow Gibbs-Thomson Effect

Eutectic Solidification (Kinetics)

: $\Delta T \rightarrow$ a) formation of interface + b) solute redistribution

How many α/β interfaces per unit length?

$\rightarrow 1/\lambda \times 2$



a) Formation of interface: ΔG

For an interlamellar spacing, λ , there is a total of $(2/\lambda) \text{ m}^2$ of α/β interface per m^3 of eutectic.

$$\Delta G = \Delta\mu \cong \frac{L\Delta T}{T_m}$$

$$\rightarrow \Delta G = \Delta\mu = \frac{2\gamma}{\lambda} \times V_m$$

Molar volume

Driving force for nucleation = Total interfacial E of eutectic phase

For very large values of λ , interfacial E ~ 0

No interface (ideal case)

$$\lambda \rightarrow \infty, \quad \Delta G(\infty) = \Delta\mu = \frac{\Delta H \Delta T_0}{T_E}$$

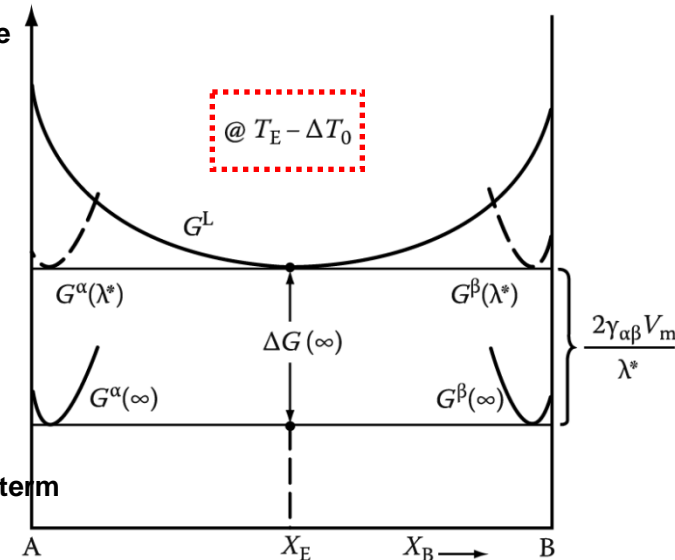
Total undercooling

With interface (real case)

$$\Delta G(\lambda) = ? = -\Delta G(\infty) + \frac{2\gamma V_m}{\lambda}$$

Interfacial E term

Solidification will take place if ΔG is negative (-).



a) All $\Delta T \rightarrow$ use for interface formation = min. λ

What would be the minimum λ ?

Critical spacing, $\lambda^* : \Delta G(\lambda^*) = 0$

최소 층상 간격

$$\Delta G(\infty) = \frac{2\gamma V_m}{\lambda^*}$$

$$\lambda^* = + \frac{2T_E \gamma V_m}{\Delta H \Delta T_0}$$

Gibbs-Thomson effect

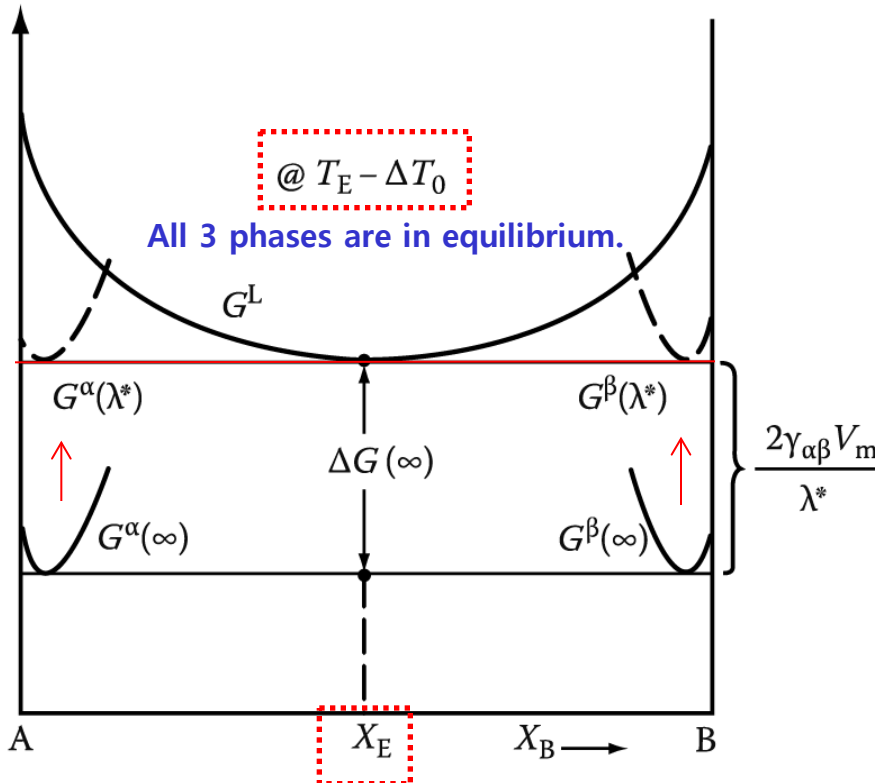
$$\lambda^* = -\frac{2T_E \gamma V_m}{\Delta H \Delta T_0} \rightarrow \text{identical to critical radius of dendrite tip in pure metal}$$

$$\text{cf) } r^* = \frac{2\gamma_{SL}}{\Delta G_V} = \left(\frac{2\gamma_{SL} T_m}{L_V} \right) \frac{1}{\Delta T}$$

L_V : latent heat per unit volume
 $L = \Delta H = H^L - H^S$

* **Growth Mechanism: Gibbs-Thomson effect in a ΔG -composition diagram?**

1) At $\lambda = \lambda^*$ ($< \infty$),



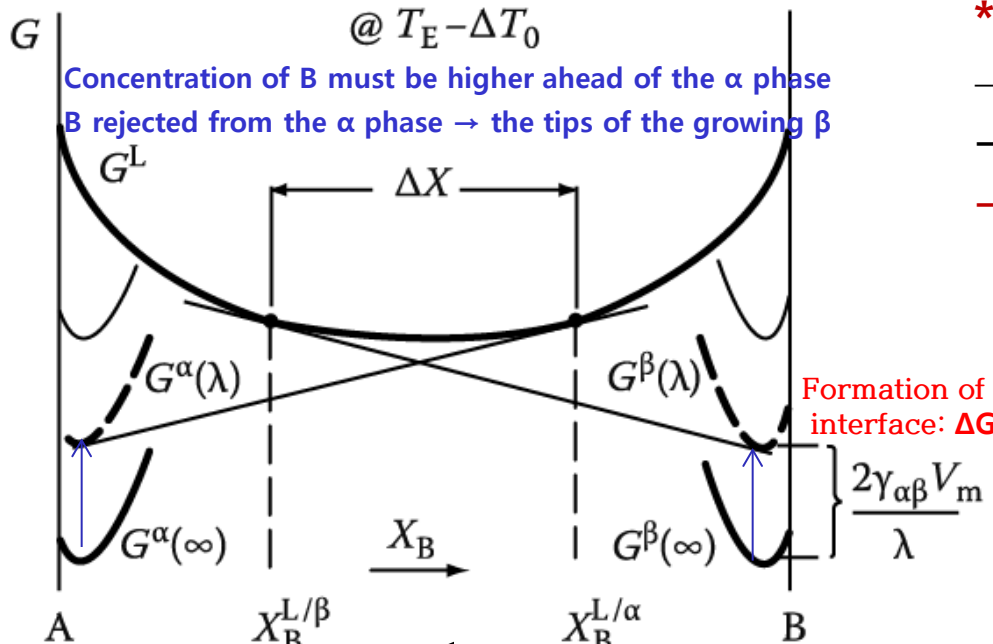
The cause of **G increase** is the curvature of the α/L and β/L interfaces arising from the need to **balance the interfacial tensions at the $\alpha/\beta/L$ triple point**, therefore the increase will be different for the two phases, but for simple cases it can be shown to be

$$\frac{2\gamma_{\alpha\beta}V_m}{\lambda} \text{ for both.}$$

1) If $\lambda = \lambda^*$, growth rate will be **infinitely slow** because the liquid in contact with both phases has the same composition, X_E in Figure 4.32.

2) At $\lambda = (\infty >) \lambda (> \lambda^*)$,

If $\infty > \lambda > \lambda^*$, G_α and G_β are correspondingly reduced because less free energy is locked in the interfaces. $\rightarrow X_B^{L/\alpha} > X_B^{L/\beta}$



* Eutectic growth rate, v

- \rightarrow if α/L and β/L interfaces are highly mobile
- \rightarrow proportional to flux of solute through liquid
- \rightarrow **diffusion controlled process**

$$v \propto D \frac{dC}{dl} \propto (X_B^{L/\alpha} - X_B^{L/\beta})$$

$$\propto 1/\text{effective diffusion distance.. } 1/\lambda$$

$$v = k_1 D \frac{\Delta X}{\lambda} \quad (1)$$

$$\lambda = \lambda^*, \Delta X = 0$$

$$\lambda = \infty, \Delta X = \Delta X_0$$

(next page)

$$\Delta X = \Delta X_0 \left(1 - \frac{\lambda^*}{\lambda}\right) \quad (2)$$

$$\Delta X_0 \propto \Delta T_0 \quad (3)$$

$$(2)+(3) \rightarrow (1) \quad v = k_2 D \frac{\Delta T_0}{\lambda} \left(1 - \frac{\lambda^*}{\lambda}\right)$$

Maximum growth rate at a fixed $\Delta T_0 \rightarrow \lambda = 2\lambda^*$

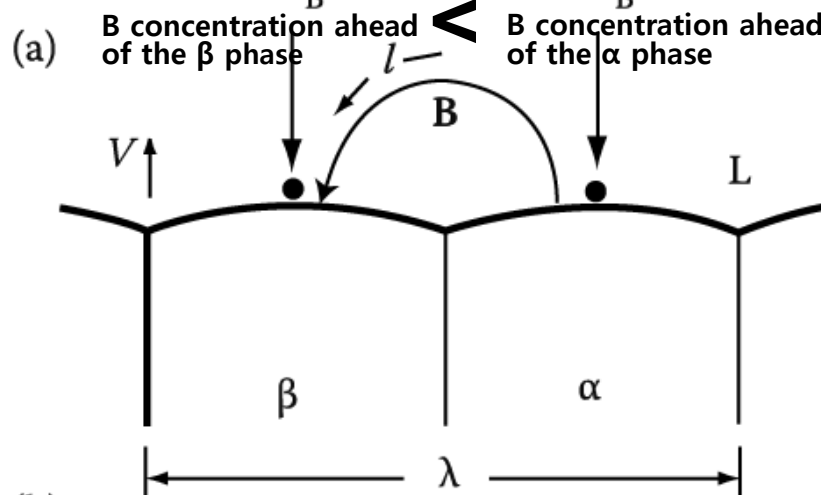


Fig. 4.33 (a) Molar free energy diagram at $(T_E - \Delta T_0)$ for the case $\lambda^* < \lambda < \infty$, showing the composition difference available to drive diffusion through the liquid (ΔX). (b) Model used to calculate the growth rate.

ΔX will it self depend on λ . \sim maximum value, ΔX_0

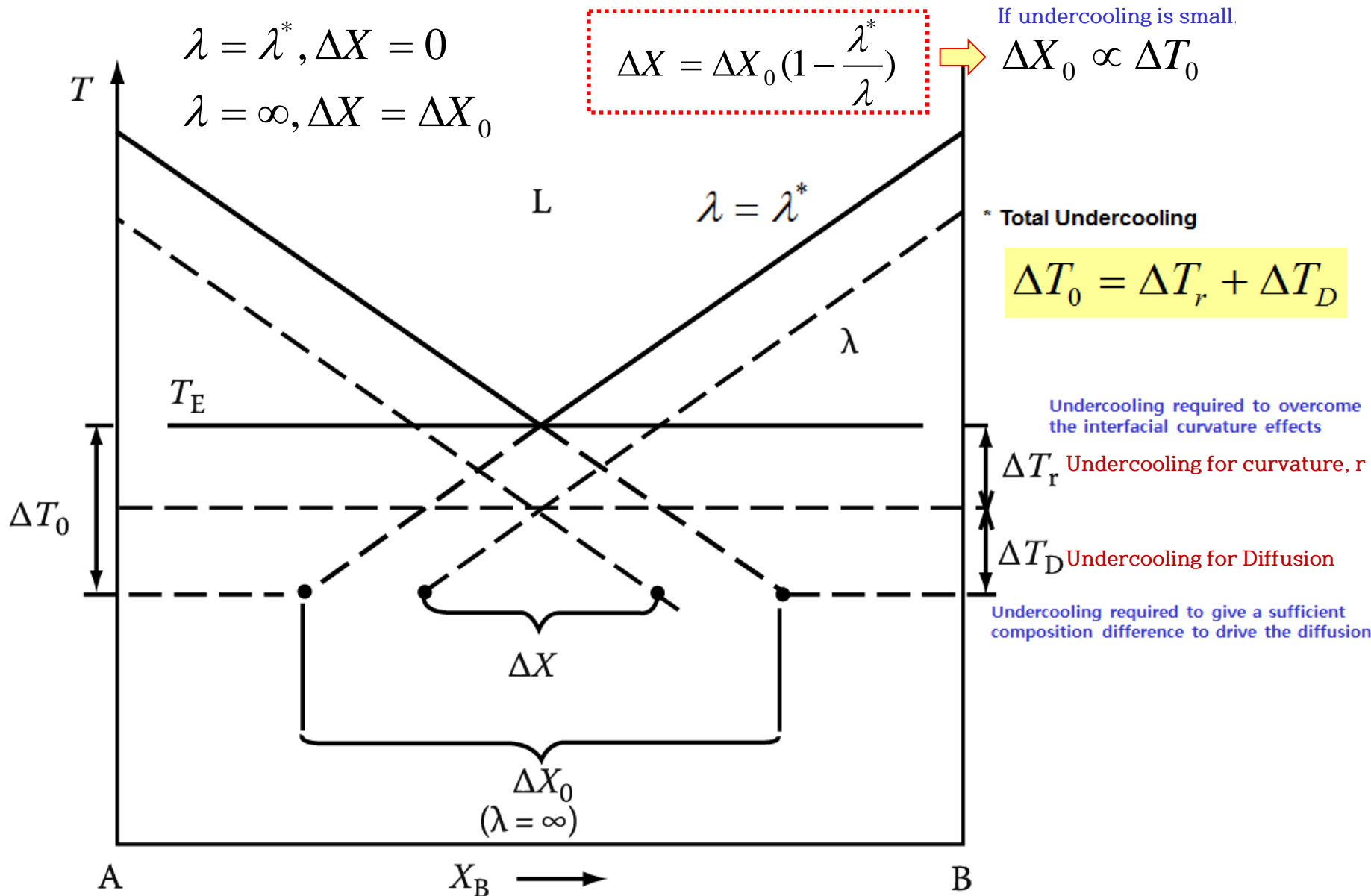
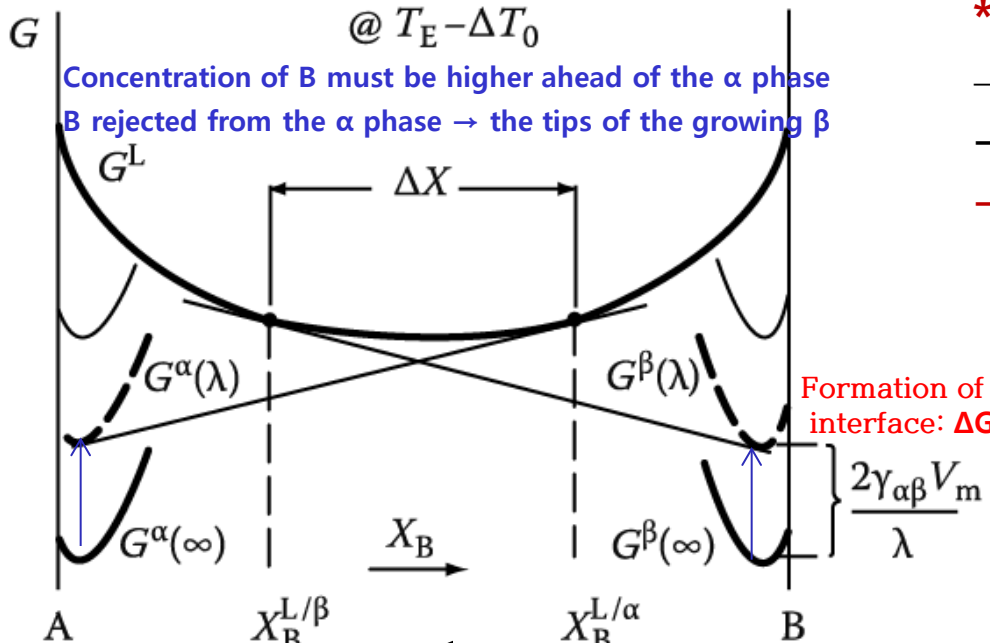


Fig. 4.34 Eutectic phase diagram showing the relationship between ΔX and ΔX_0 (exaggerated for clarity)

2) At $\lambda = (\infty >) \lambda (> \lambda^*)$,

If $\infty > \lambda > \lambda^*$, G_α and G_β are correspondingly reduced because less free energy is locked in the interfaces. $\rightarrow X_B^{L/\alpha} > X_B^{L/\beta}$



*** Eutectic growth rate, v**

- \rightarrow if α/L and β/L interfaces are highly mobile
- \rightarrow proportional to flux of solute through liquid
- \rightarrow **diffusion controlled process**

$$v \propto D \frac{dC}{dl} \propto (X_B^{L/\alpha} - X_B^{L/\beta})$$

$$\propto 1/\text{effective diffusion distance.. } 1/\lambda$$

$$v = k_1 D \frac{\Delta X}{\lambda} \quad (1)$$

$$\lambda = \lambda^*, \Delta X = 0$$

$$\lambda = \infty, \Delta X = \Delta X_0$$

(next page)

$$\Delta X = \Delta X_0 \left(1 - \frac{\lambda^*}{\lambda}\right) \quad (2)$$

$$\Delta X_0 \propto \Delta T_0 \quad (3)$$

$$(2)+(3) \rightarrow (1) \quad v = k_2 D \frac{\Delta T_0}{\lambda} \left(1 - \frac{\lambda^*}{\lambda}\right)$$

Maximum growth rate at a fixed $\Delta T_0 \rightarrow \lambda = 2\lambda^*$

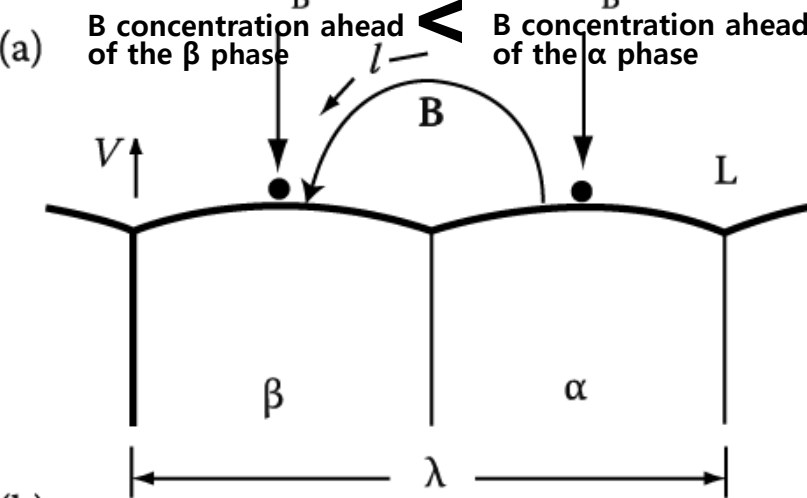


Fig. 4.33 (a) Molar free energy diagram at $(T_E - \Delta T_0)$ for the case $\lambda^* < \lambda < \infty$, showing the composition difference available to drive diffusion through the liquid (ΔX). (b) Model used to calculate the growth rate.

Closer look at the tip of a growing dendrite

different from a planar interface because heat can be conducted away from the tip in three dimensions.

Assume the solid is isothermal ($T'_S = 0$)

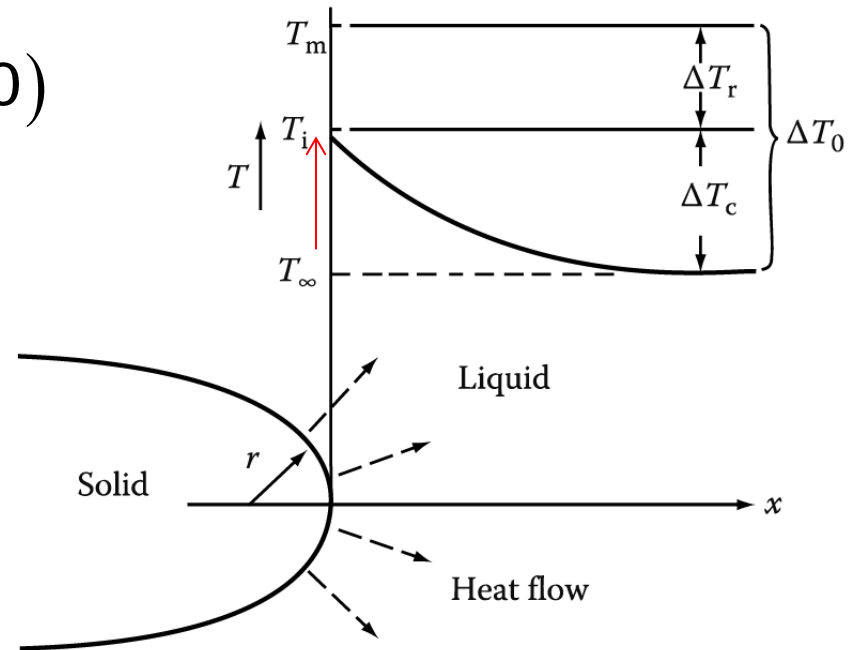
From $K_S T'_S = K_L T'_L + v L_V$

If $T'_S = 0$, $v = \frac{-K_L T'_L}{L_V}$

A solution to the heat-flow equation for a hemispherical tip:

$$T'_L (\text{negative}) \cong \frac{\Delta T_C}{r} \quad \Delta T_C = T_i - T_\infty$$

$$v = \frac{-K_L T'_L}{L_V} \cong \frac{K_L}{L_V} \cdot \frac{\Delta T_C}{r} \quad v \propto \frac{1}{r}$$



However, ΔT also depends on r .
How?

Thermodynamics at the tip?

Gibbs-Thomson effect:
melting point depression

$$\Delta G = \frac{L_V}{T_m} \Delta T_r = \frac{2\gamma}{r} \quad \Delta T_r = \frac{2\gamma T_m}{L_V r}$$

Minimum possible radius (r)?

$$r_{min} : \Delta T_r \rightarrow \Delta T_0 = T_m - T_\infty \rightarrow r^*$$

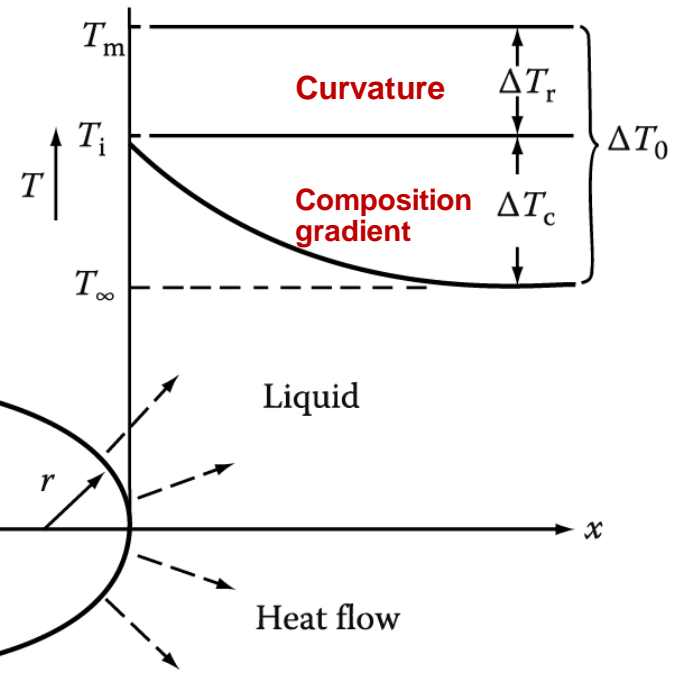
The crit.nucl.radius

$$r^* = \frac{2\gamma T_m}{L_v \Delta T_0}$$

$$\Delta T_r = \frac{2\gamma T_m}{L_v r}$$

Express ΔT_r by r , r^* and ΔT_0 .

$$\Delta T_r = \frac{r^*}{r} \Delta T_0$$



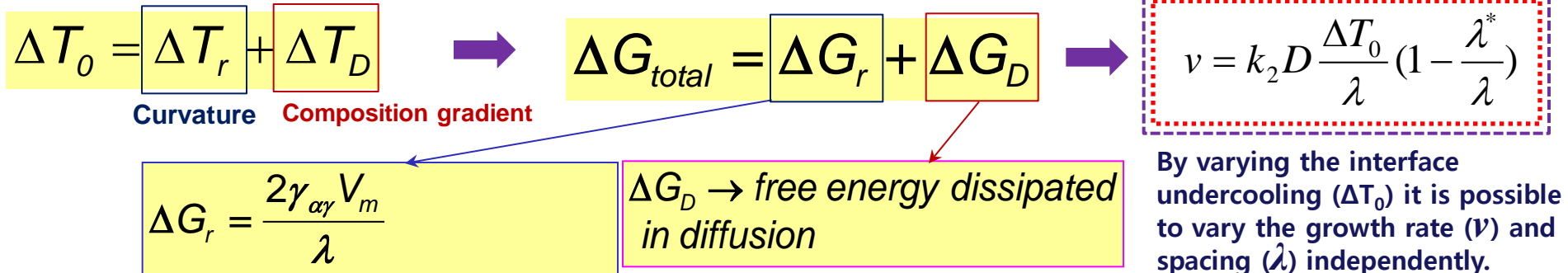
$$v \cong \frac{K_L}{L_v} \cdot \frac{\Delta T_c}{r} = \frac{K_L}{L_v} \cdot \frac{(\Delta T_0 - \Delta T_r)}{r} = \frac{K_L}{L_v} \cdot \frac{\Delta T_0}{r} \left(1 - \frac{r^*}{r} \right)$$

$v \rightarrow 0$ as $r \rightarrow r^*$ due to Gibbs-Thomson effect
as $r \rightarrow \infty$ due to slower heat conduction

Maximum velocity?

$$\rightarrow r = 2r^*$$

Undercooling ΔT_0



Therefore, it is impossible to predict the spacing that will be observed for a given growth rate. **However, controlled growth experiments show that a specific value of λ is always associated with a given growth rate.**

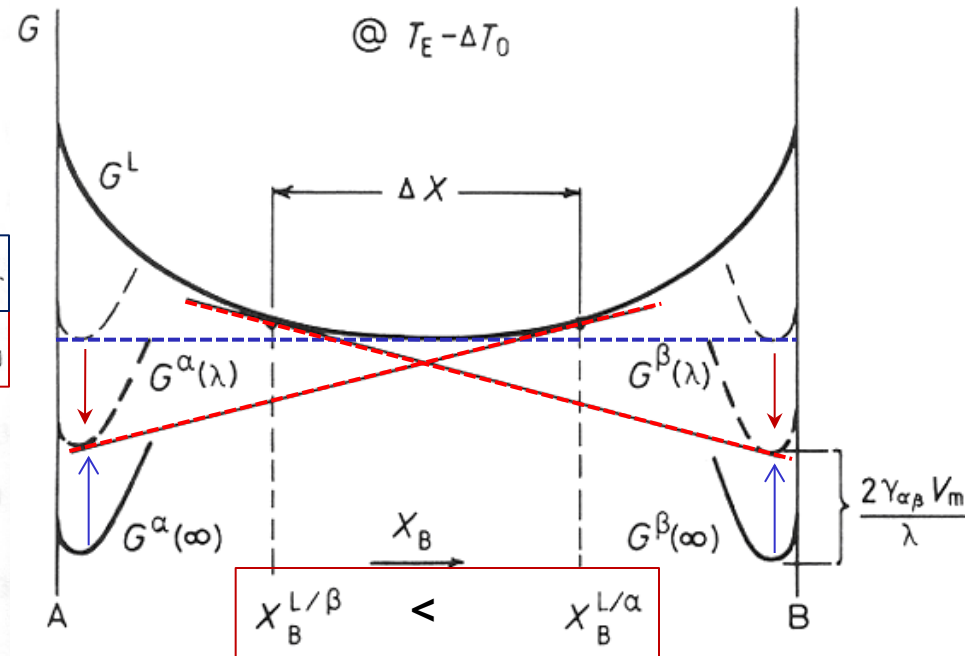
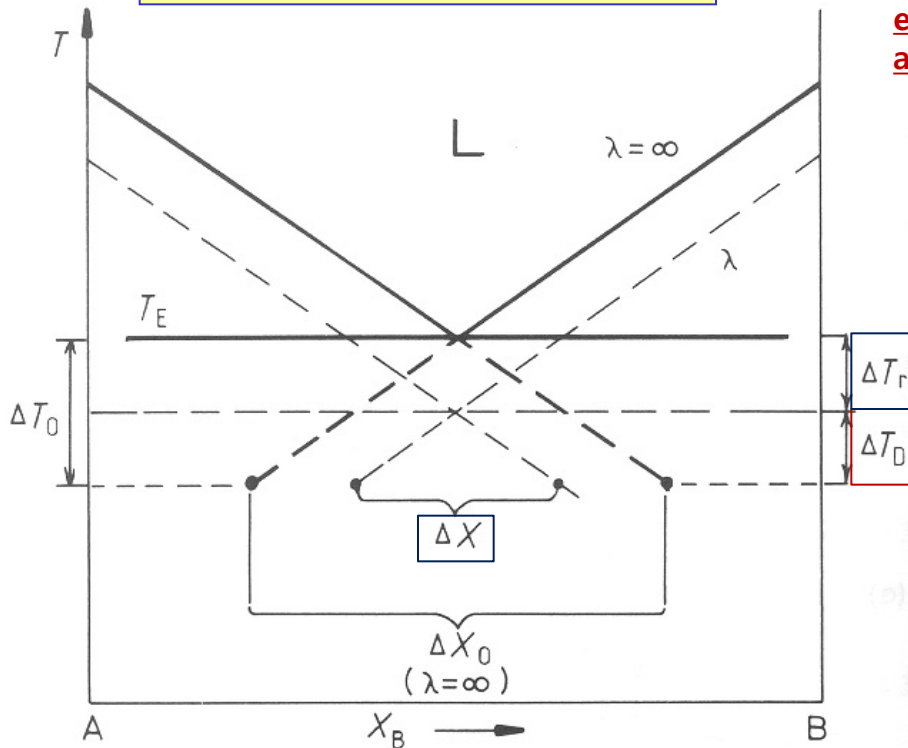
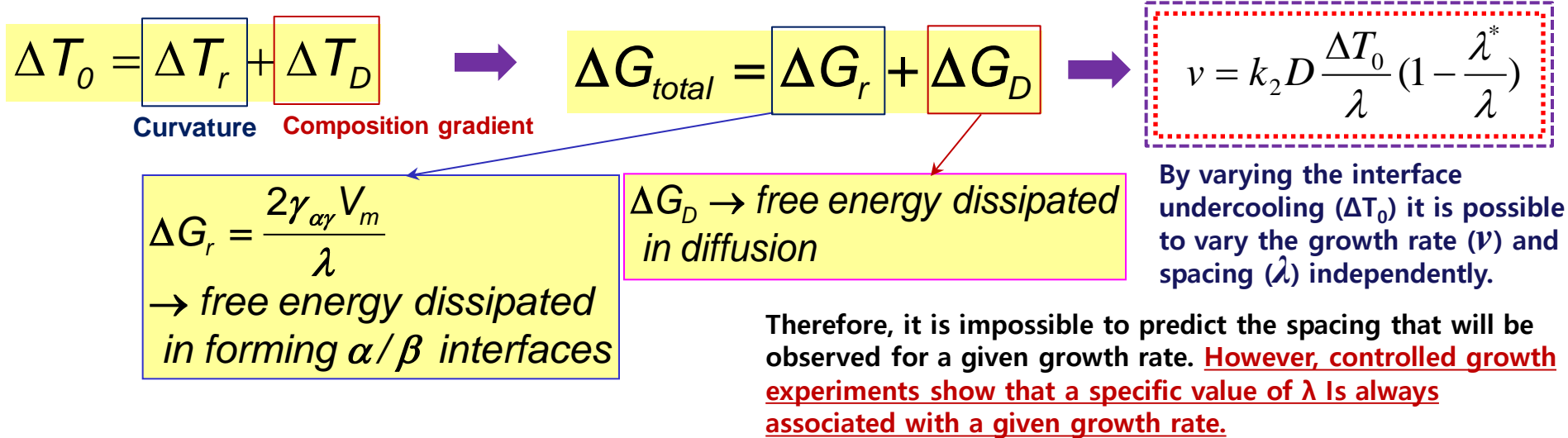


Fig. 4.34 Eutectic phase diagram showing the relationship between ΔX and ΔX_0 (exaggerated for clarity)

Undercooling ΔT_0



* For example,

Maximum growth rate at a fixed $\Delta T_0 \rightarrow \lambda_0 = 2\lambda^*$

(4) $v = k_2 D \frac{\Delta T_0}{\lambda} \left(1 - \frac{\lambda^*}{\lambda}\right)$

(5) $v_0 = k_2 D \Delta T_0 / 4\lambda^*$

From Eq. 4.39

$\lambda^* = + \frac{2T_E \gamma V_m}{\Delta H \Delta T_0}$

(6) $\Delta T_0 \propto 1 / \lambda^*$

So that the following relationships are predicted:

(5) + (6)

$v_0 \lambda_0^2 = k_3$ (constant)

$\frac{v_0}{(\Delta T_0)^2} = k_4$

Ex) Lamellar eutectic in the Pb-Sn system

$k_3 \sim 33 \mu\text{m}^3/\text{s}$ and $k_4 \sim 1 \mu\text{m}/\text{s}\cdot\text{K}^2$

$\rightarrow v = 1 \mu\text{m}/\text{s}, \lambda_0 = 5 \mu\text{m}$ and $\Delta T_0 = 1 \text{ K}$

* Total Undercooling

$$\Delta T_0 = \Delta T_r + \Delta T_D$$

Strictly speaking, ΔT_i term should be added but, negligible for high mobility interfaces
 Driving force for atom migration across the interfaces

Undercooling required to overcome the interfacial curvature effects

Undercooling required to give a sufficient composition difference to drive the diffusion

$\Delta T_D \rightarrow$ Vary continuously from the middle of the α to the middle of the β lamellae

$\Delta T_0 = const \leftarrow$ Interface is essentially isothermal.

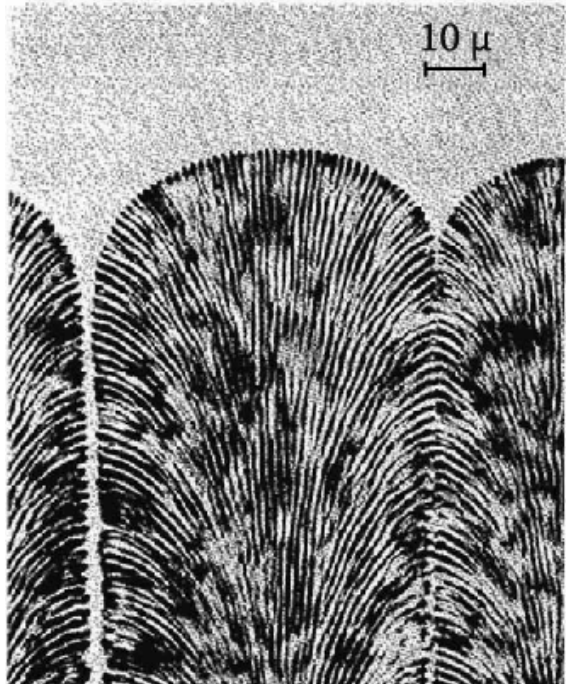
$\Delta T_D \rightarrow \Delta T_r$ The interface curvature will change across the interface.
 Should be compensated

* A planar eutectic front is not always stable.

Binary eutectic alloys contains impurities or other alloying elements \rightarrow "Form a cellular morphology"
 analogous to single phase solidification restrict in a sufficiently high temp. gradient.

\rightarrow The solidification direction changes as the cell walls are approached and the lamellar or rod structure fans out and may even change to an irregular structure.

\rightarrow Impurity elements (here, mainly copper) concentrate at the cell walls.



A planar eutectic front is not always stable.

Binary eutectic alloys contains **impurities** or **other alloying elements** → **“Form a cellular morphology”** analogous to single phase solidification restrict in a sufficiently high temp. gradient.

- The solidification direction changes as the cell walls are approached and the lamellar or rod structure fans out and may even change to an irregular structure.
- **Impurity elements (here, mainly copper) concentrate at the cell walls.**

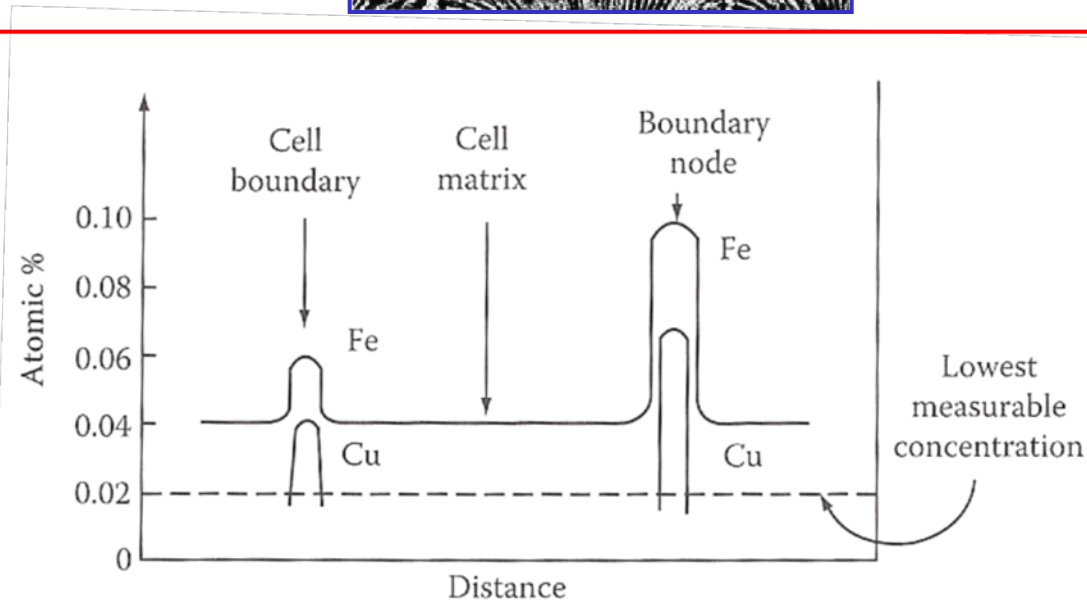
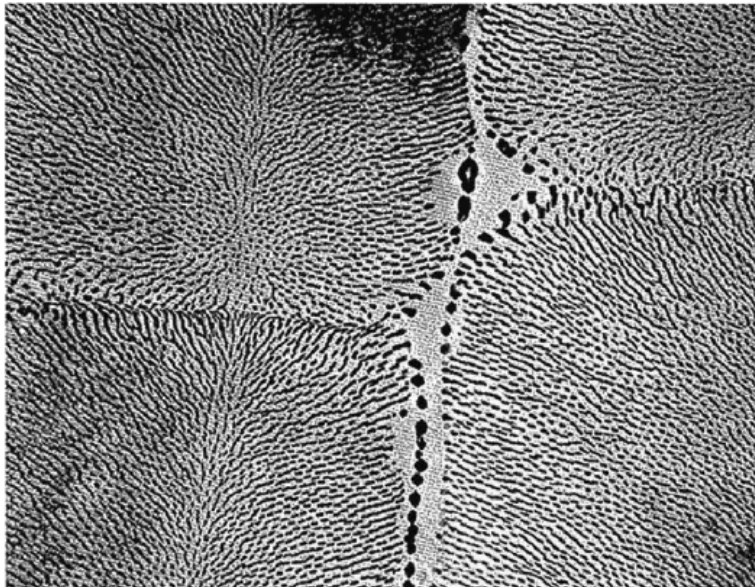
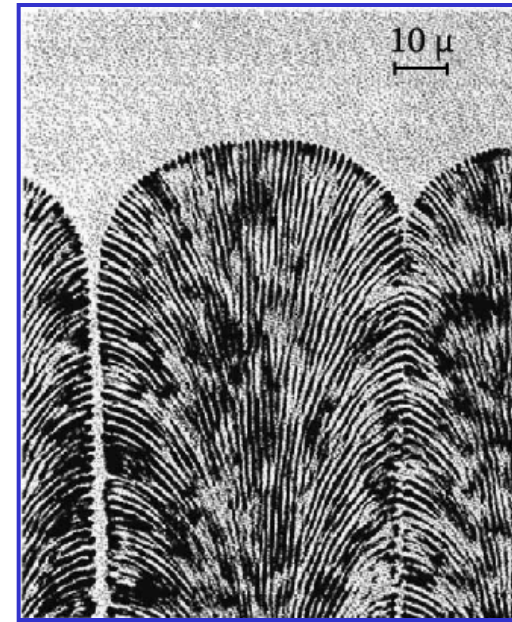


Fig. 4.35 Transverse section through the cellular structure of an Al-Al₆Fe rod eutectic (x3500).

Fig. 4.36 Composition profiles across the cells in Fig. 4.35b.

Q: Off-eutectic Solidification?

4.3.3 Off-eutectic Solidification _Pb-Sn system

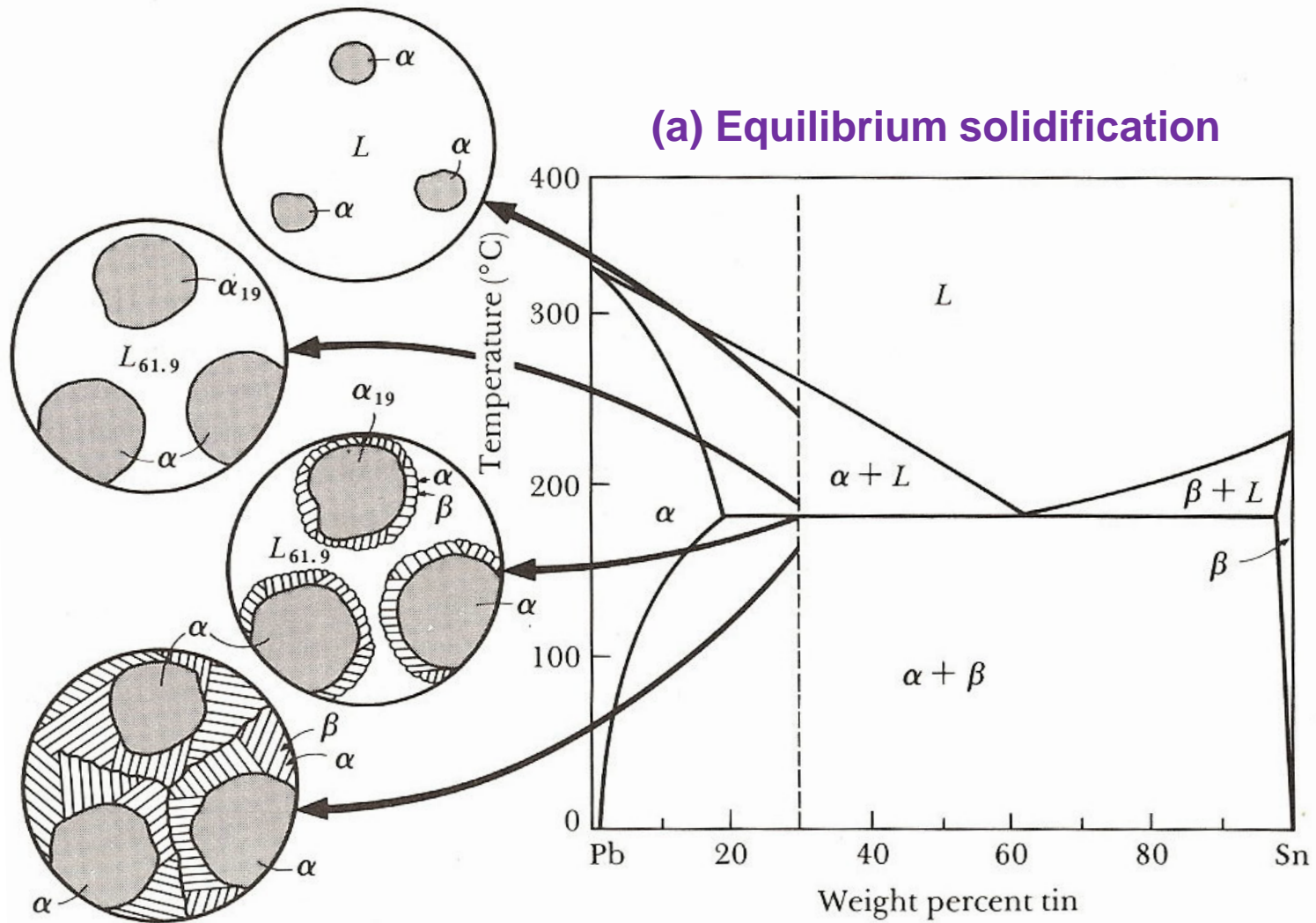
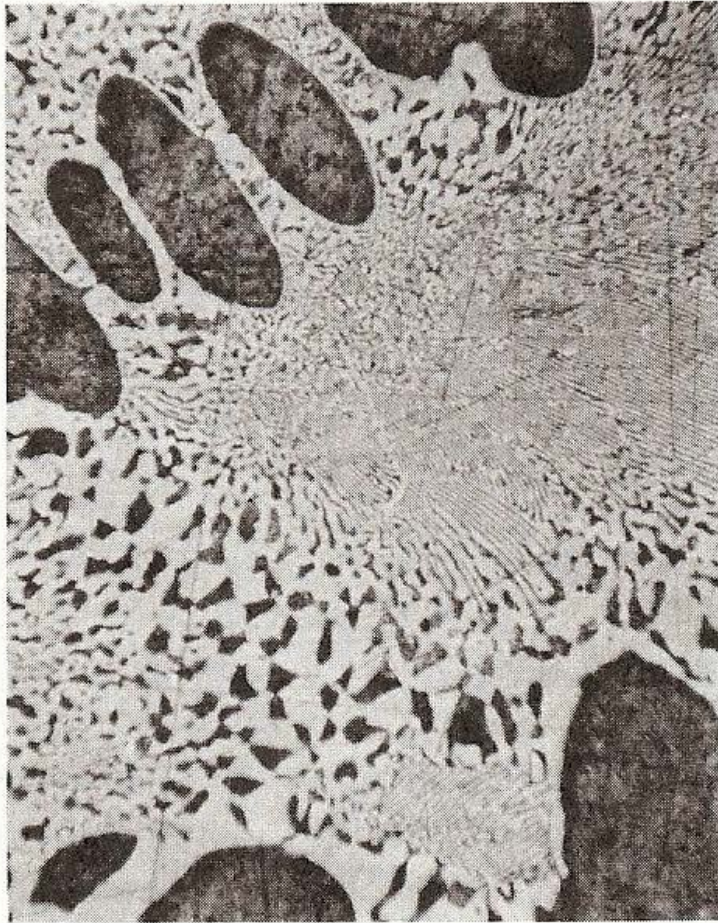
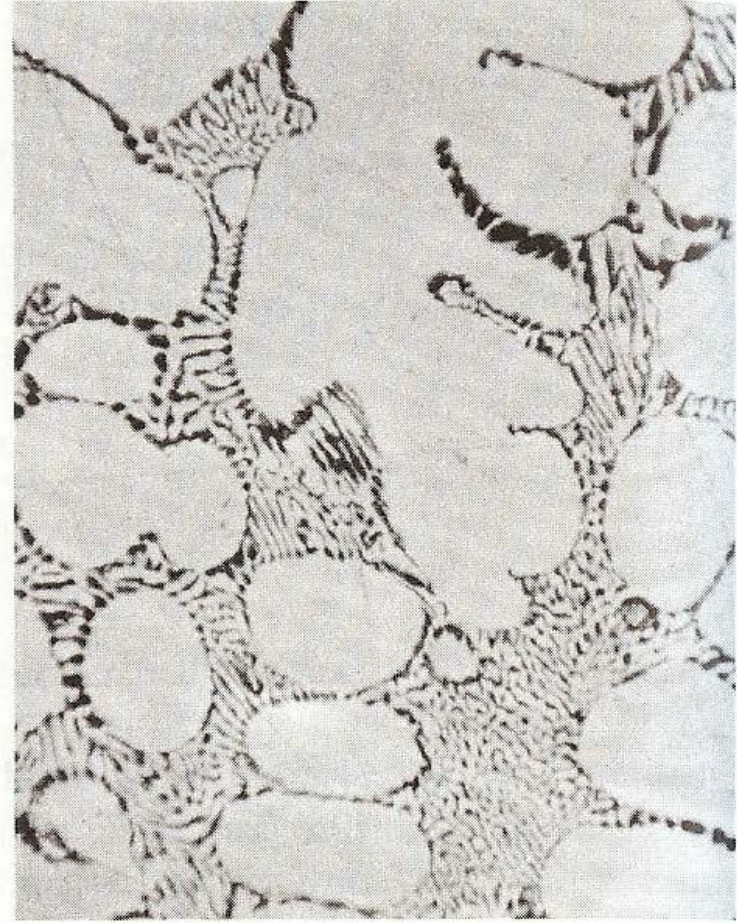


FIGURE 10-12 The solidification and microstructure of a hypoeutectic alloy (Pb-30% Sn).

4.3.3 Off-eutectic Solidification _Pb-Sn system



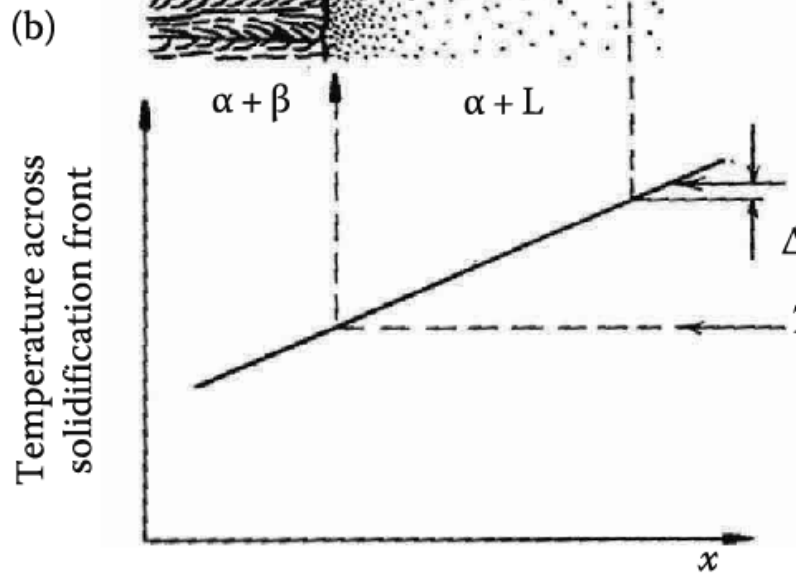
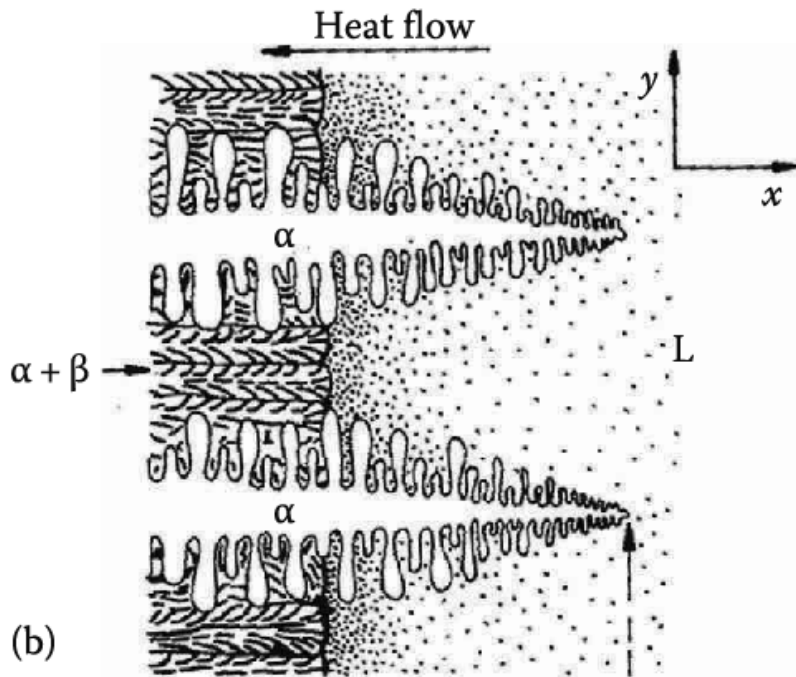
(a)



(b)

FIGURE 10-13 (a) A hypoeutectic lead-tin alloy. (b) A hypereutectic lead-tin alloy. The dark constituent is the lead-rich solid α , the light constituent is the tin-rich solid β , and the fine plate structure is the eutectic ($\times 400$).

4.3.3 Off-eutectic Solidification



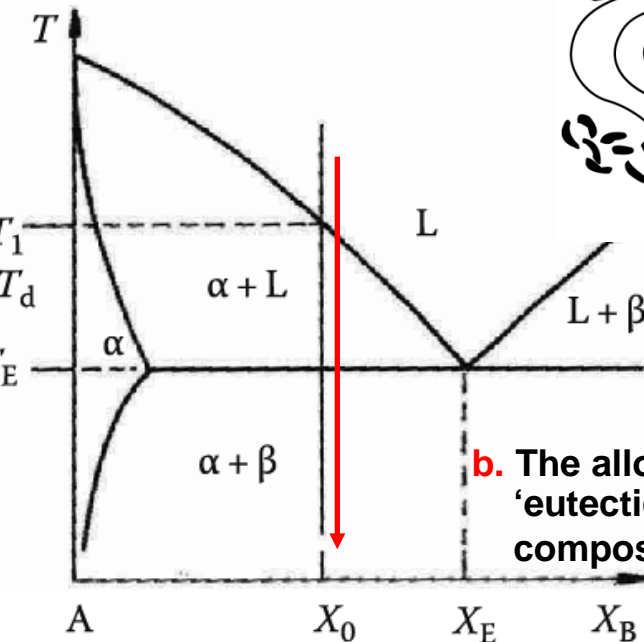
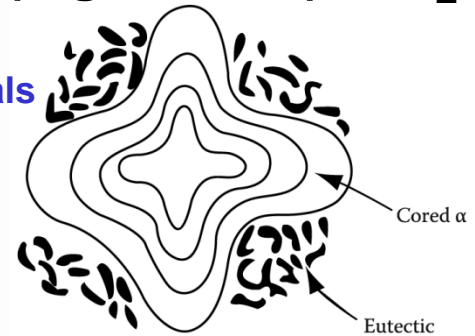
(b) Non-equilibrium solidification

a. primary α + eutectic lamellar

- Primary α dendrites form at T_1 . Rejected solute increases X_L to X_E ; eutectic solidification follows.

- **Coring**: primary α (low solute) at T_1 and the eutectic (high solute) at T_E .

→ in-situ composite materials



b. The alloy solidifies as 100% 'eutectic' with an overall composition X_0 instead of X_E .

(c)

(a)

Q: Peritectic Solidification ($L + \alpha \rightarrow \beta$)?

Solidification and microstructure that develop as a result of the **peritectic reaction**

(a) Equilibrium solidification

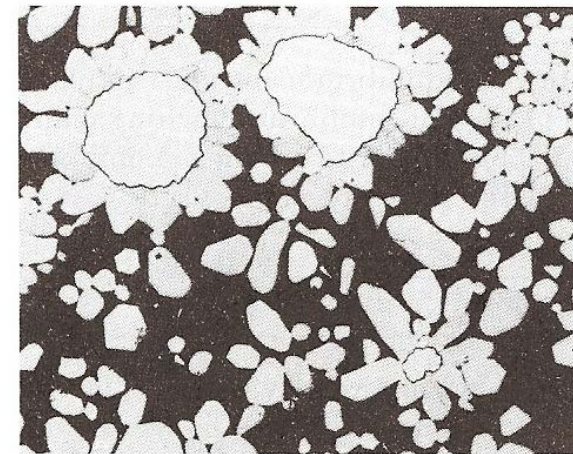
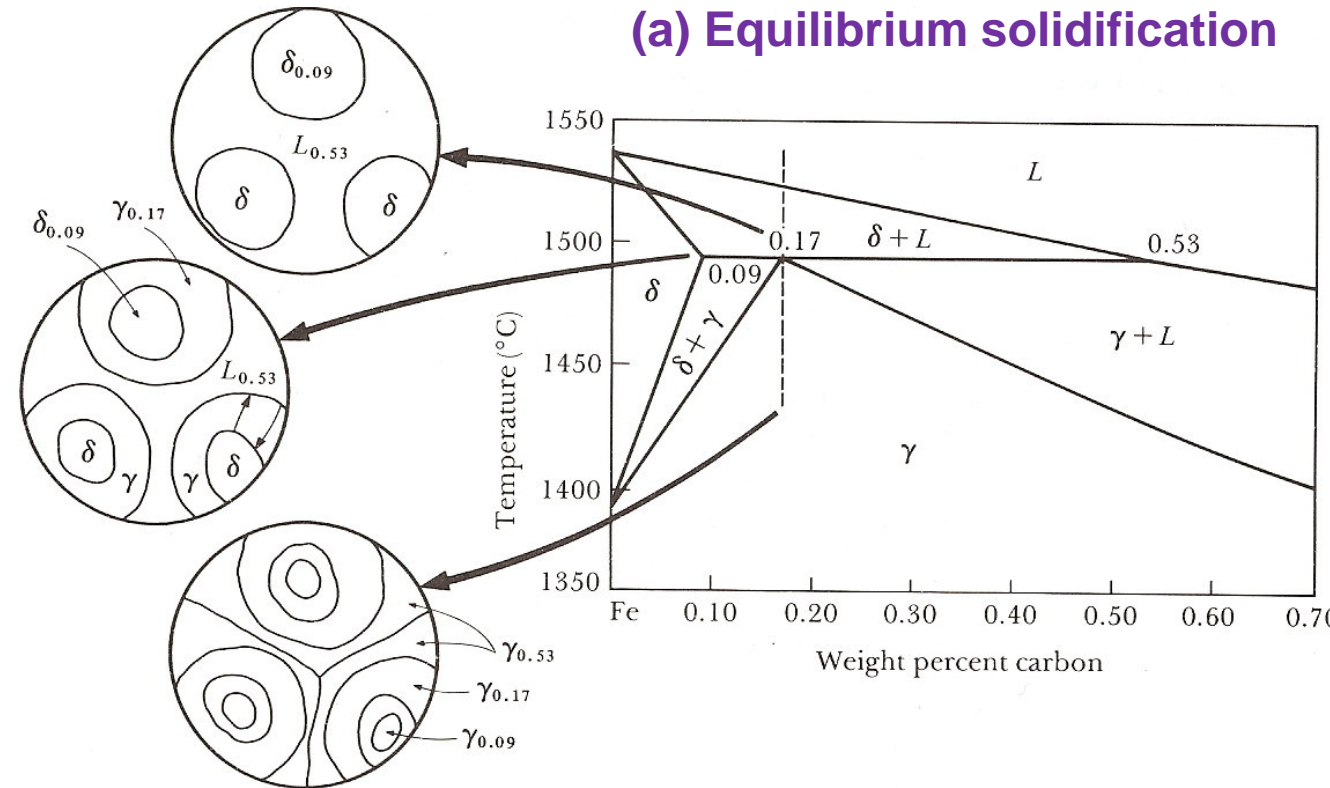
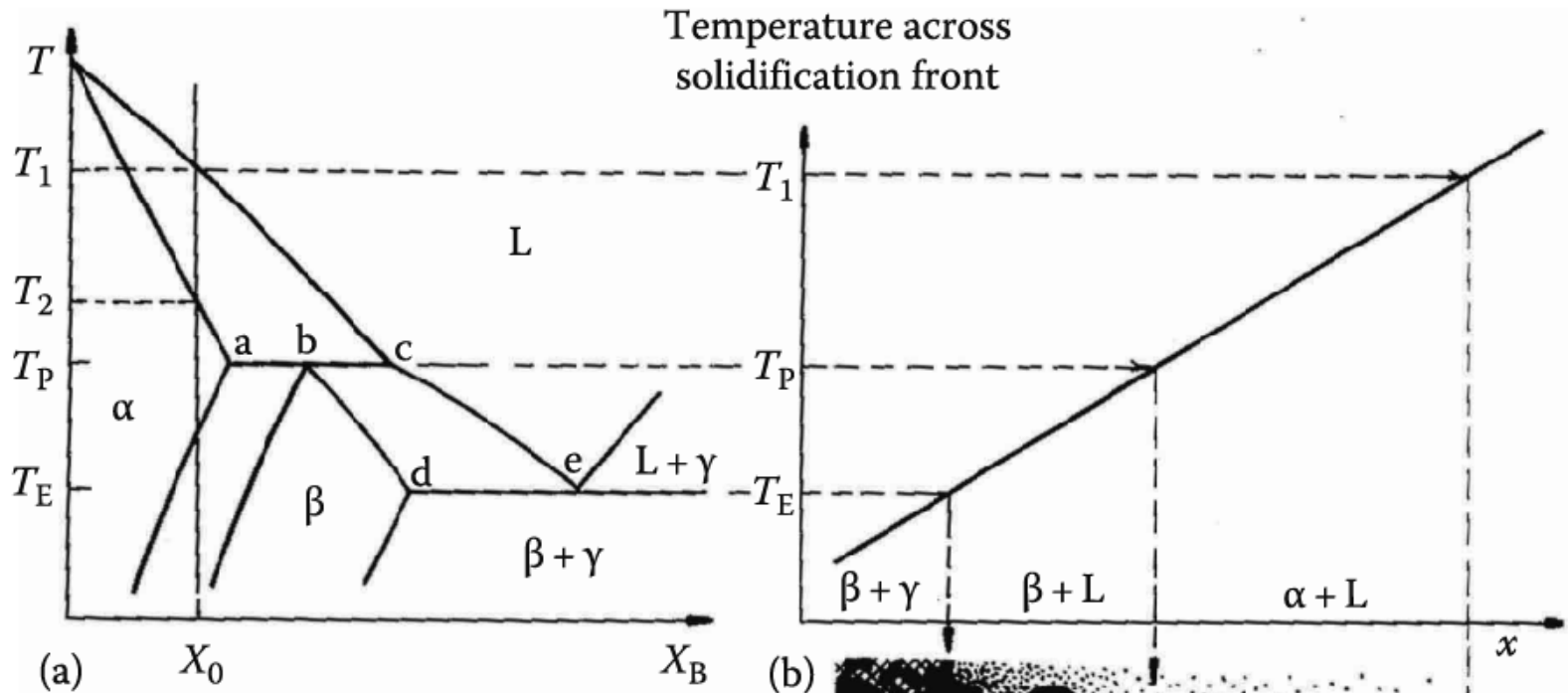


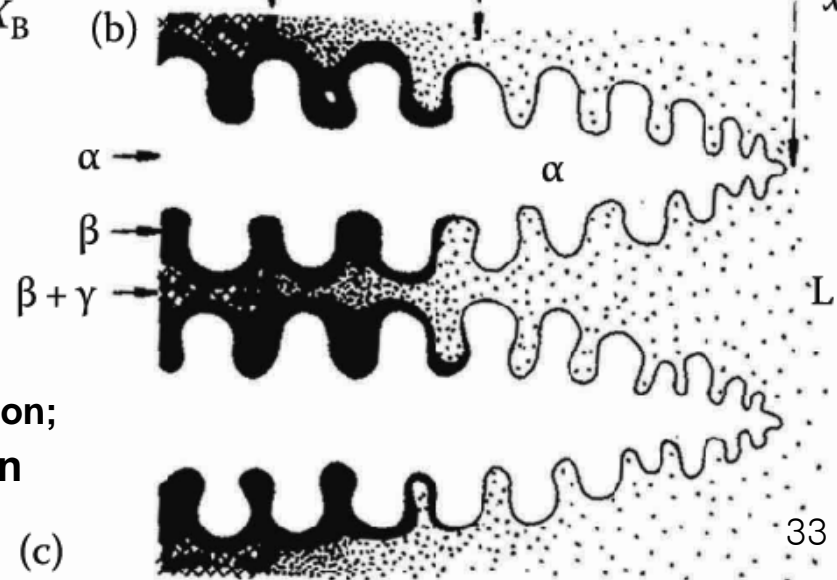
FIGURE 10-24 The peritectic reaction in a Cd-10% Cu alloy begins when rounded

4.3.4 Peritectic Solidification



(b) Non-equilibrium solidification

- $L + \alpha \rightarrow \beta$, difficult to complete.
- α dendrites first form at T_1 ;
Liquid reaches the composition 'c';
 β forms as the result of the peritectic reaction;
 α coring is isolated from further reaction
finally $\beta + \gamma$ eutectic forms.



**Two of the most important application of solidification :
“Casting” and “Weld solidification”**

Q: What kinds of ingot structure exist?

Ingot Structure

- **Chill zone**
- **Columnar zone**
- **Equiaxed zone**

4.4 Solidification of **Ingots** and **Castings**

a lump of metal, usually shaped like a brick.

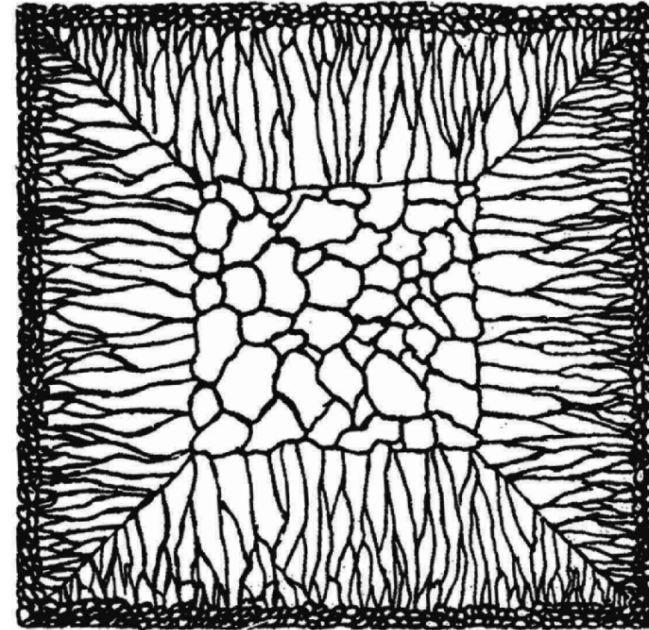
Later to be worked, e.g. by rolling, extrusion or forging > blank (small)

an object or piece of machinery which has been made by pouring a liquid such as hot metal into a container

Permitted to regain their shape afterwards, or reshaped by machining

Ingot Structure

- **outer Chill zone**
: equiaxed crystals
- **Columnar zone**
: elongated or column-like grains
- **central Equiaxed zone**



Chill zone

- **Solid nuclei form on the mould wall and begin to grow into the liquid.**
 - 1) **If the pouring temp. is low:** liquid~ rapidly cooled below the liquidus temp. → **big-bang nucleation** → **entirely equiaxed ingot structure**, no columnar zone
 - 2) **If the pouring temp. is high:** liquid~remain above the liquidus temp. for a long time → **majority of crystals~remelt under influence of the turbulent melt ("convection current")** → **form the chill zone**

Columnar zone

After pouring the **temperature gradient** at the mould walls **decreases** and the crystals in the chill zone grow dendritically in certain crystallographic directions, e.g. **<100>** in the case of cubic metals.

→ **grow fastest and outgrow less favorably oriented neighbors**

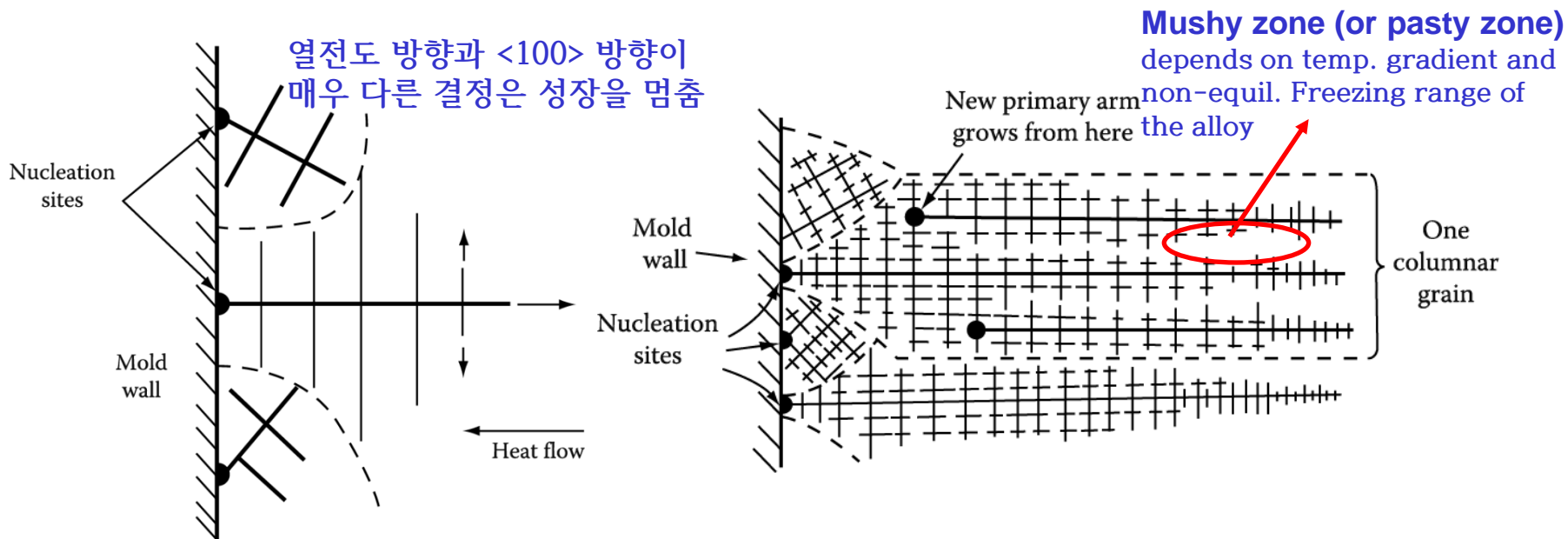
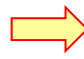


Fig. 4.41 Competitive growth soon after pouring. Dendrites with primary arms normal to the mould wall, i.e. parallel to the maximum temperature gradient, outgrow less favorably oriented neighbors.

Fig. 4.42 Favorably oriented dendrites develop into columnar grains. Each columnar grain originates from the same heterogeneous nucleation site, but can contain many primary dendrite arms.

- 1) In general, the secondary arms become coarser with distance behind the primary dendrite tips.
- 2) The primary and secondary dendrite arm spacing increase with increasing distance from the mold wall.
(\because a corresponding decrease in the cooling rate with time after pouring)

 **Mushy zone (or pasty zone)**
depends on temp. gradient and non-equil. freezing range of the alloy

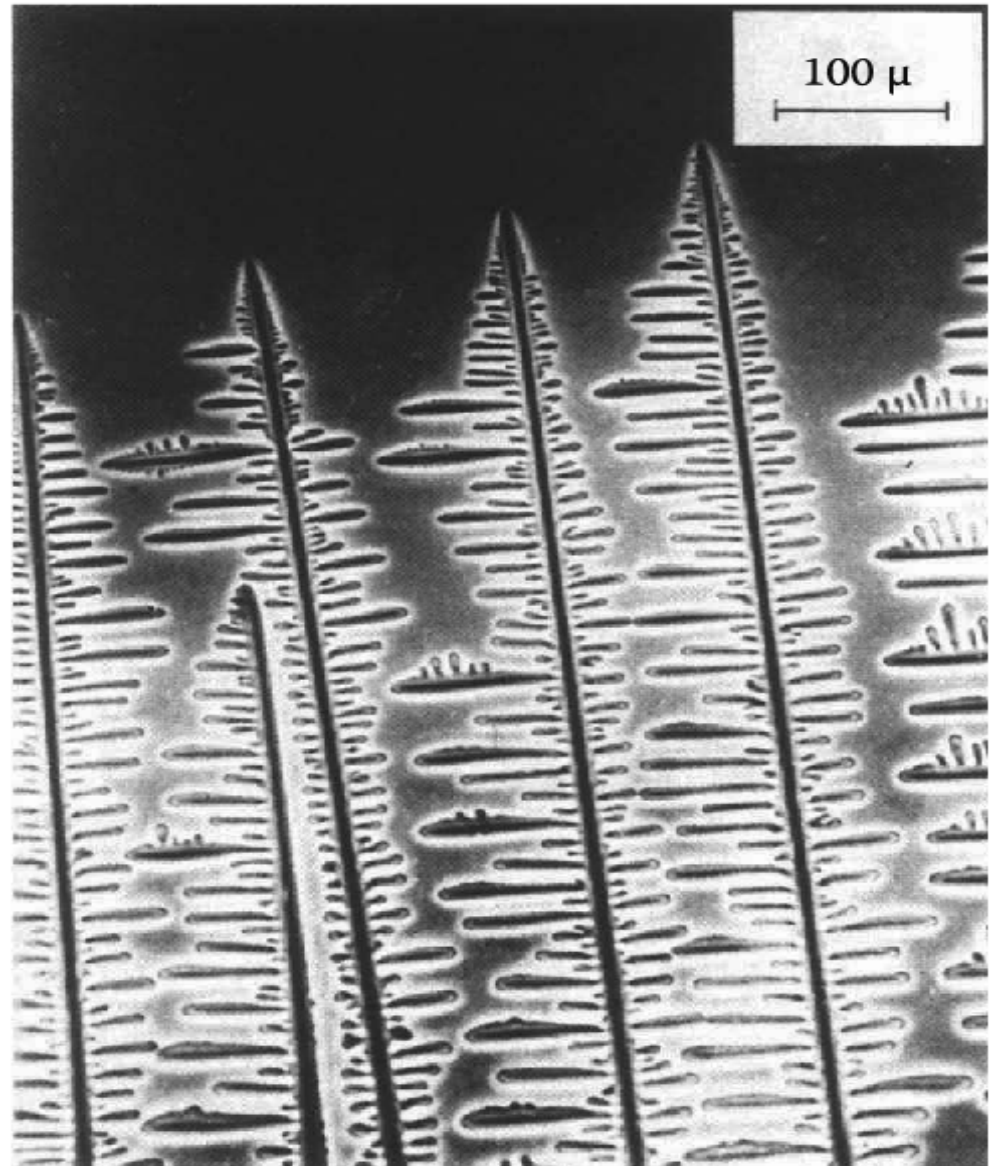


Fig. 4.28 Columnar dendrites in a transparent organic alloy.

(After K.A. Jackson in Solidification, American Society for Metals, 1971, p. 121.)

Equiaxed zone

The equiaxed zone consists of **equiaxed grains randomly** oriented in the centre of the ingot. An important origin of these grains is thought to be **melted-off dendrite side-arms + convection current**

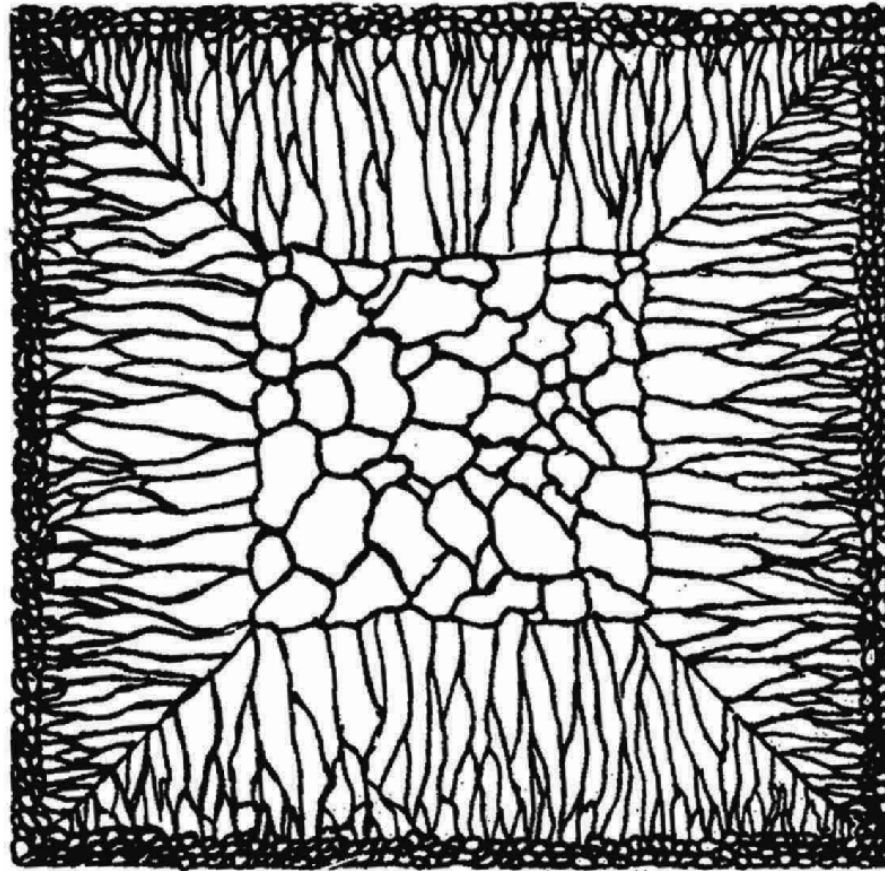
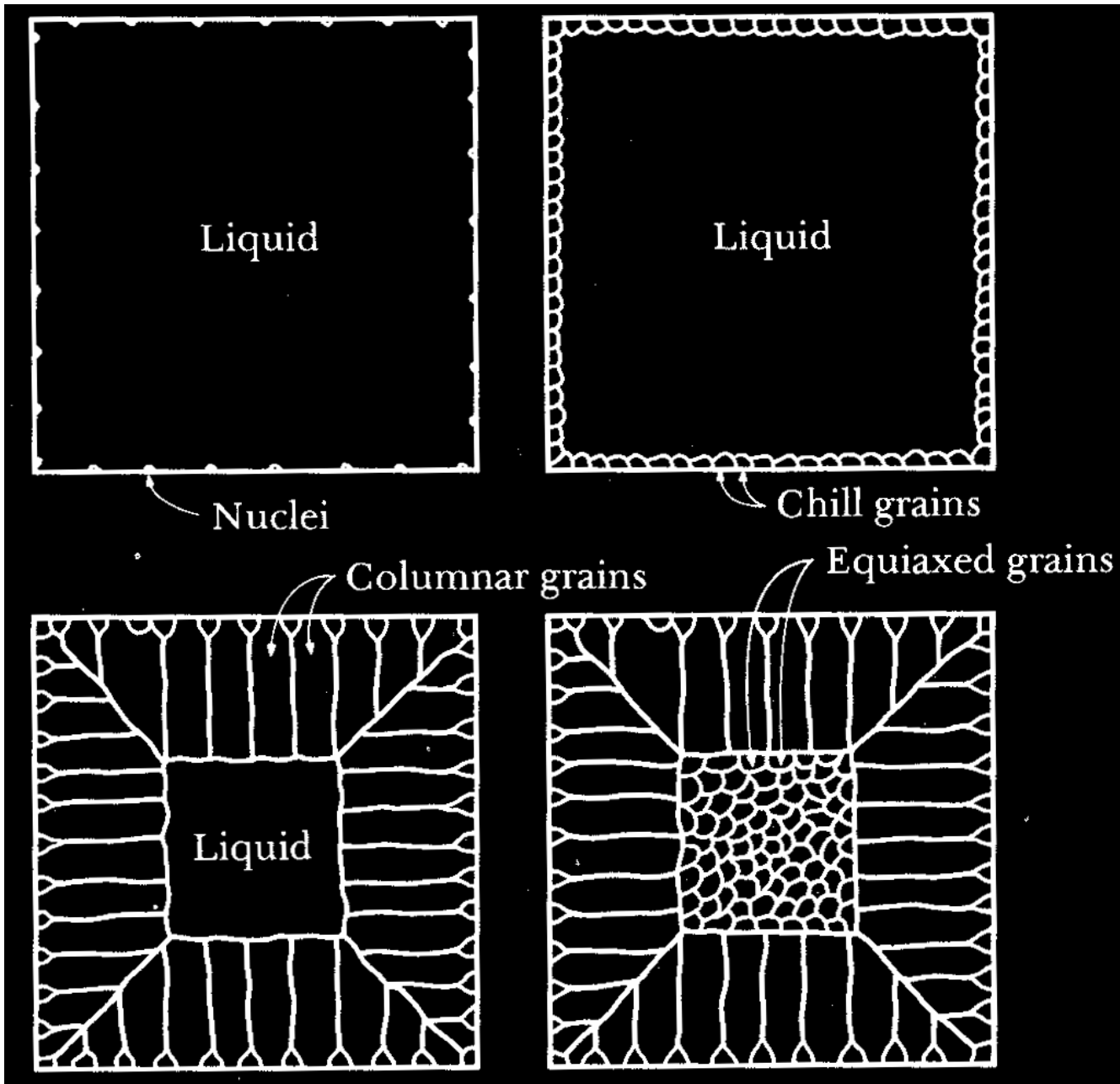


Fig. 4.40 Schematic cast grain structure.

(After M.C. Flemings, *Solidification Processing*, McGraw-Hill, New York, 1974.) 38



Q: What kind of segregations exist?

4.4.2 Segregation and Shrinkage in Ingots and Castings

(a) Segregation

- **Macrosegregation** : Large area composition changes over distances comparable to the size of the specimen.
- **Microsegregation** : In the secondary dendrite arm occur on the scale of the secondary dendrite arm spacing.

Four important factors that can lead to macrosegregation

- a) **Shrinkage** due to solidification and thermal contraction.
- b) **Density differences** in the interdendritic liquid.
- c) **Density differences** between the solid and liquid.
- d) **Convection currents** driven by temperature-induced density differences in the liquid.

Fig. Simulation of macrosegregation formation in a large steel casting, showing liquid velocity vectors during solidification (left) and final carbon macrosegregation pattern (right).

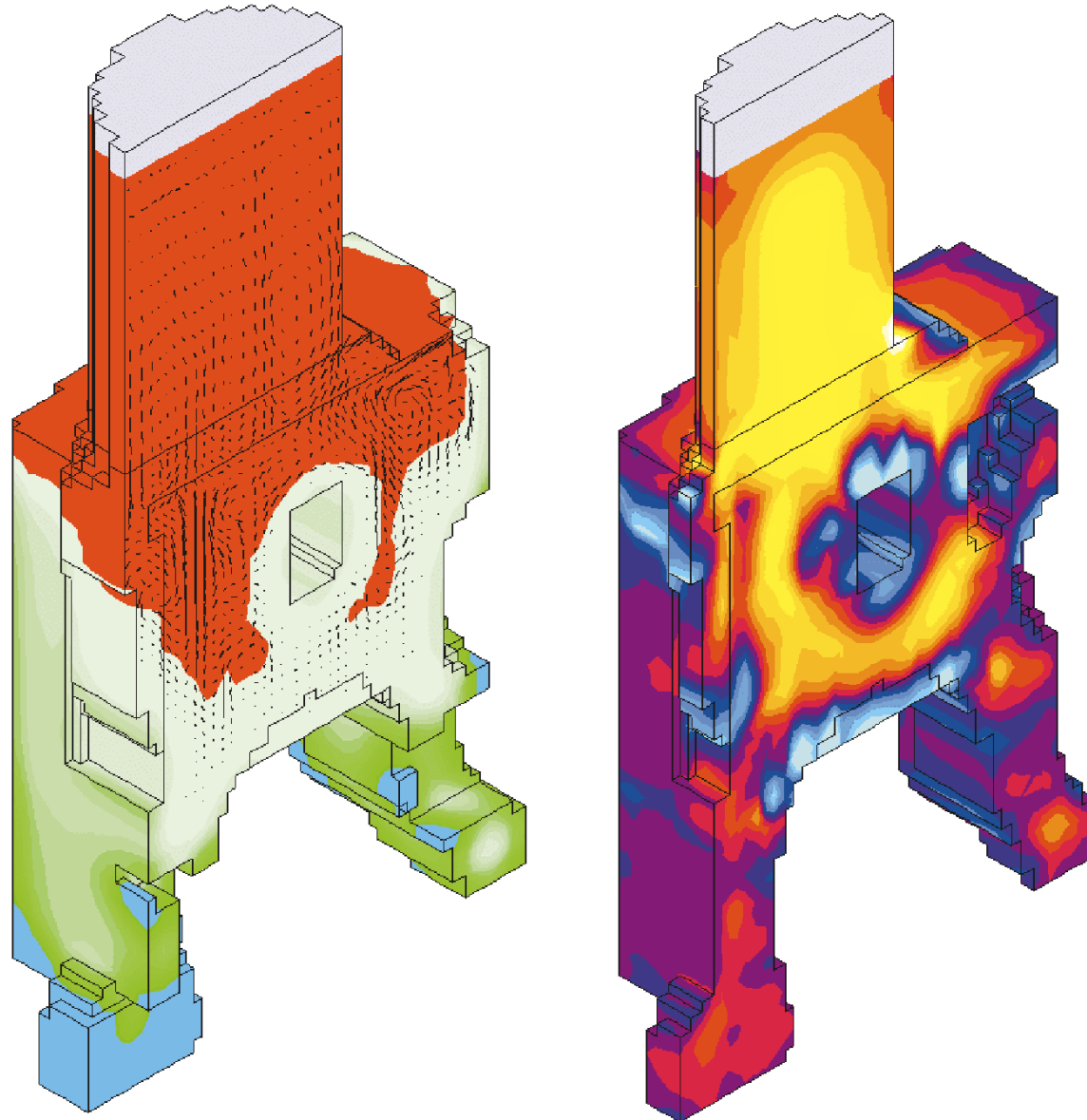


Fig.

Freckles in a single-crystal nickel-based superalloy prototype blade (left) and close-up of a single freckle (right) (courtesy of A. F. Giamei, United Technologies Research Center).

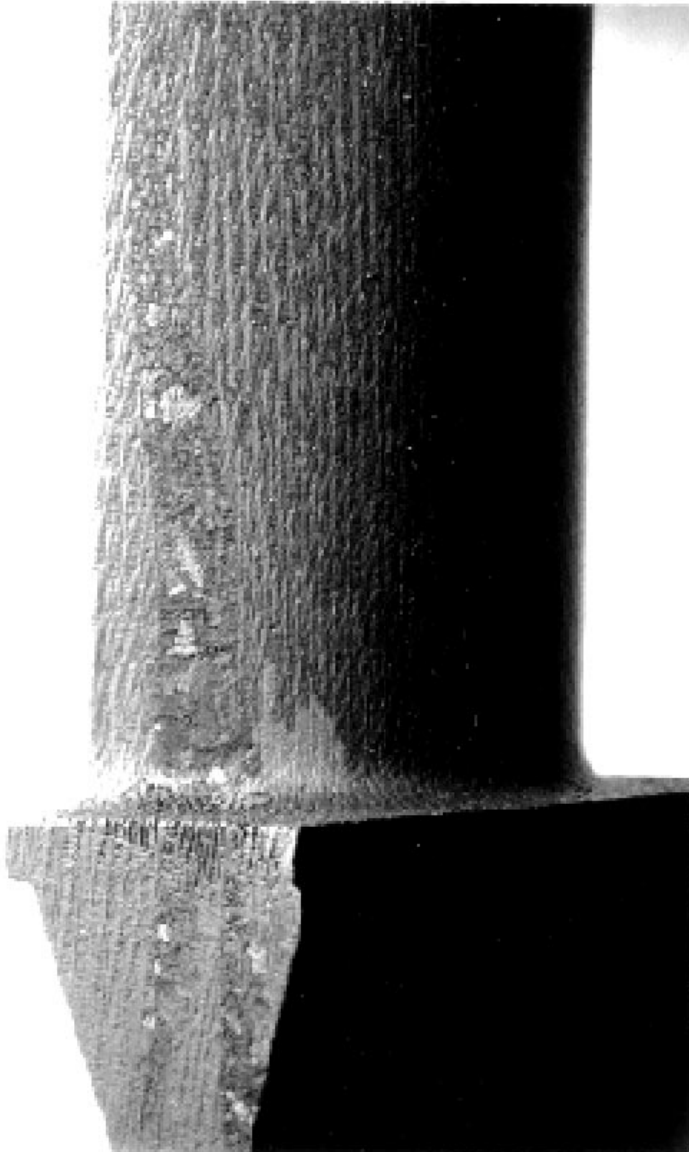
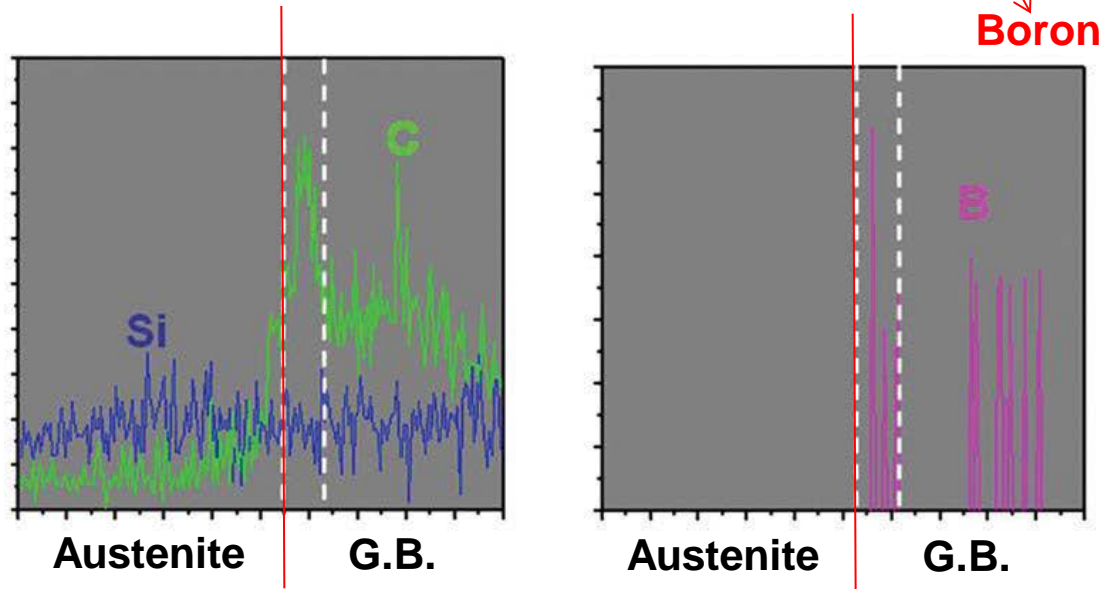
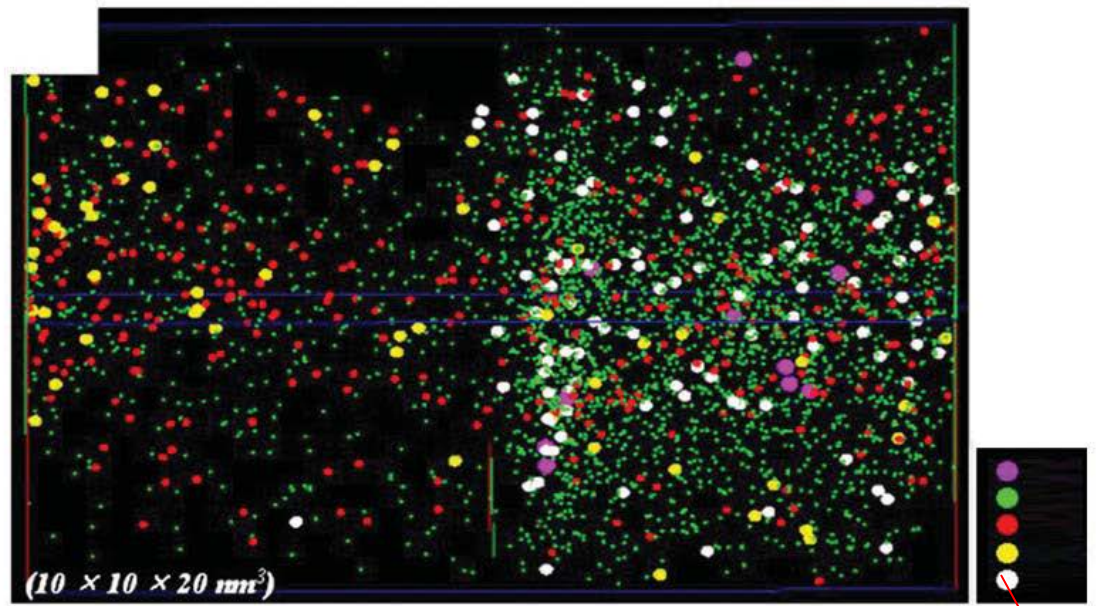
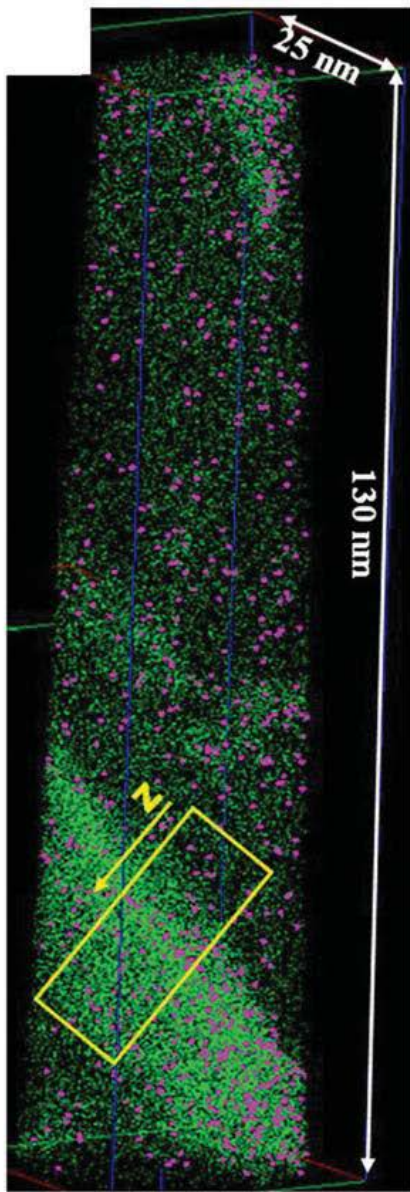


Fig.

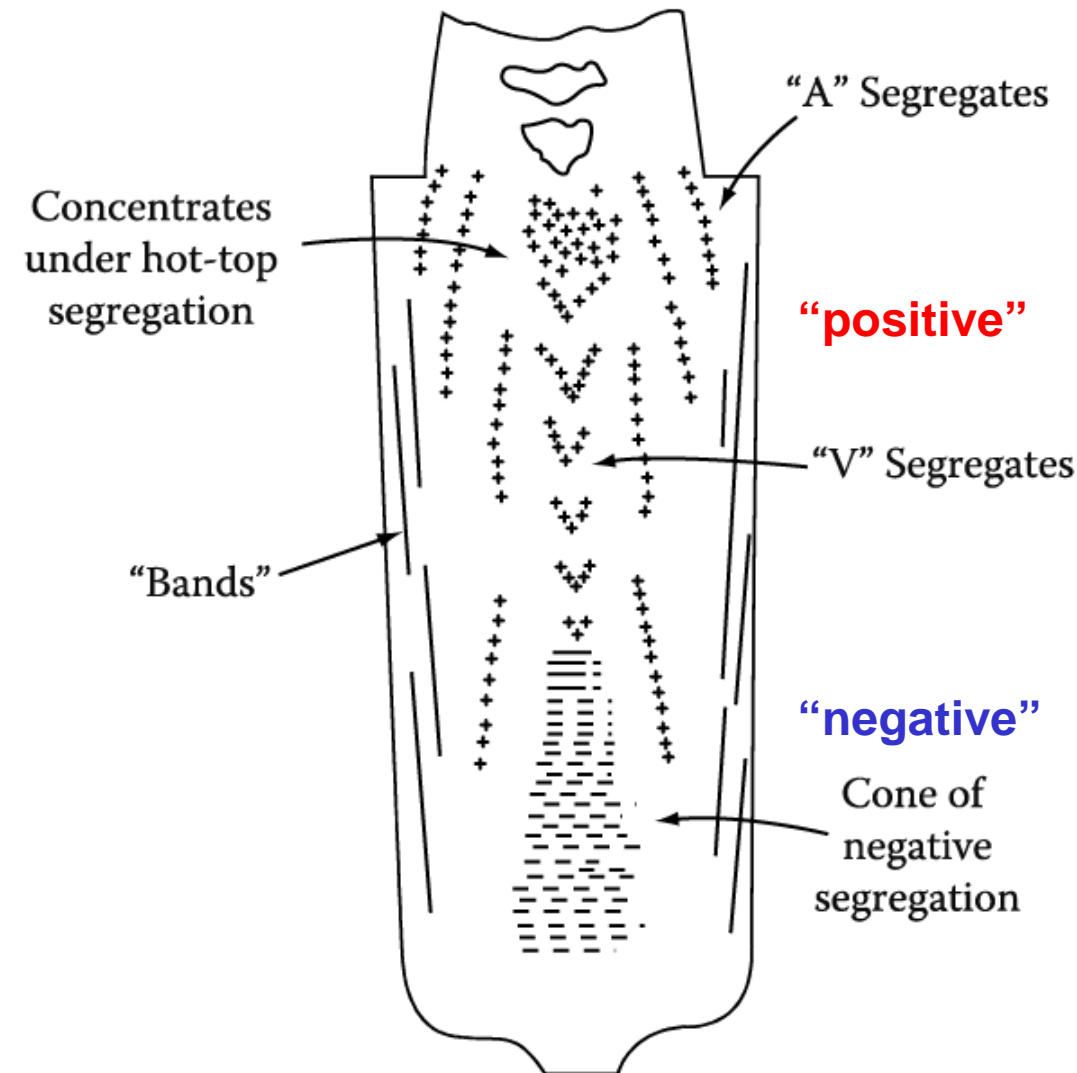
Sulfur print showing centerline segregation in a continuously cast steel slab (courtesy of IPSCO Inc.).





The result obtained by APT analysis. (a) 3D Atom map of **Boron steel containing 100 ppm Boron** and (b) composition profile showing **solute segregation within retained austenite and grain boundary**

- * **Segregation:** undesirable ~ deleterious effects on mechanical properties
 - subsequent **homogenization heat treatment**, but diffusion in the solid far too slow
 - **good control of the solidification process**



Inverse segregation (역편석): As the columnar dendrites thicken solute-rich liquid (assuming $k < 1$) must flow back between the dendrites to **compensate for (a) shrinkage** and **this raises the solute content of the outer parts of the ingot relative to the center.**

EX) Al-Cu and Cu-Sn alloys with a wide freezing range (relatively low k)

Negative segregation: The solid is usually denser than the liquid and sinks carrying with it less solute (초기응고고상) than the bulk composition (assuming $k < 1$). This can, therefore, lead to a region of negative segregation near the bottom of the ingot. ((b) Gravity effects)

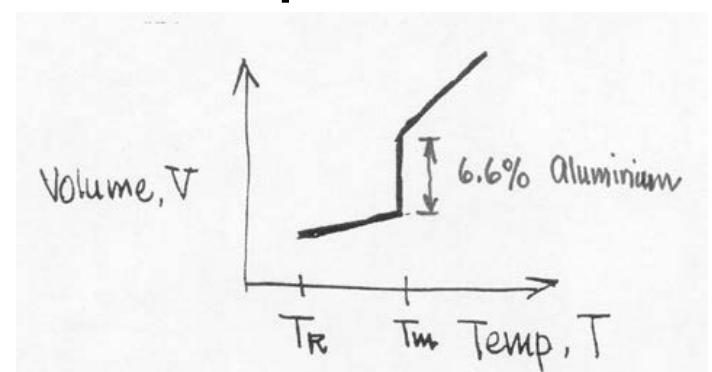
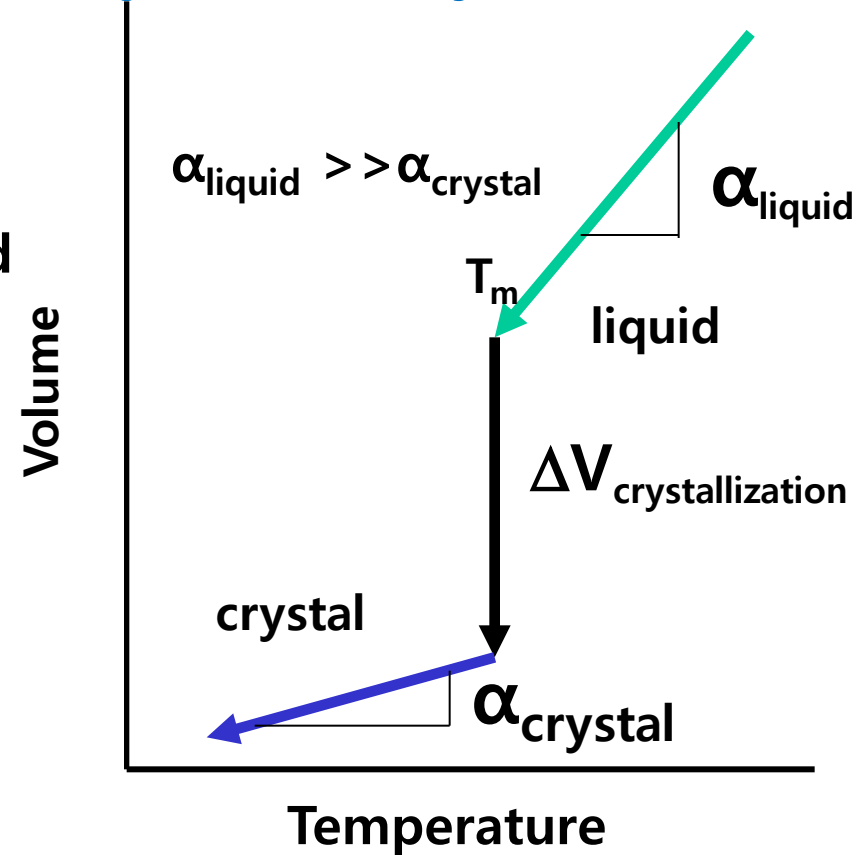
Fig. 4.43 Segregation pattern in a large killed steel ingot. + positive, - negative segregation. (After M.C. Flemings, Scandinavian Journal of Metallurgy 5 (1976) 1.) 46

Q: Shrinkage in Solidification and Cooling?

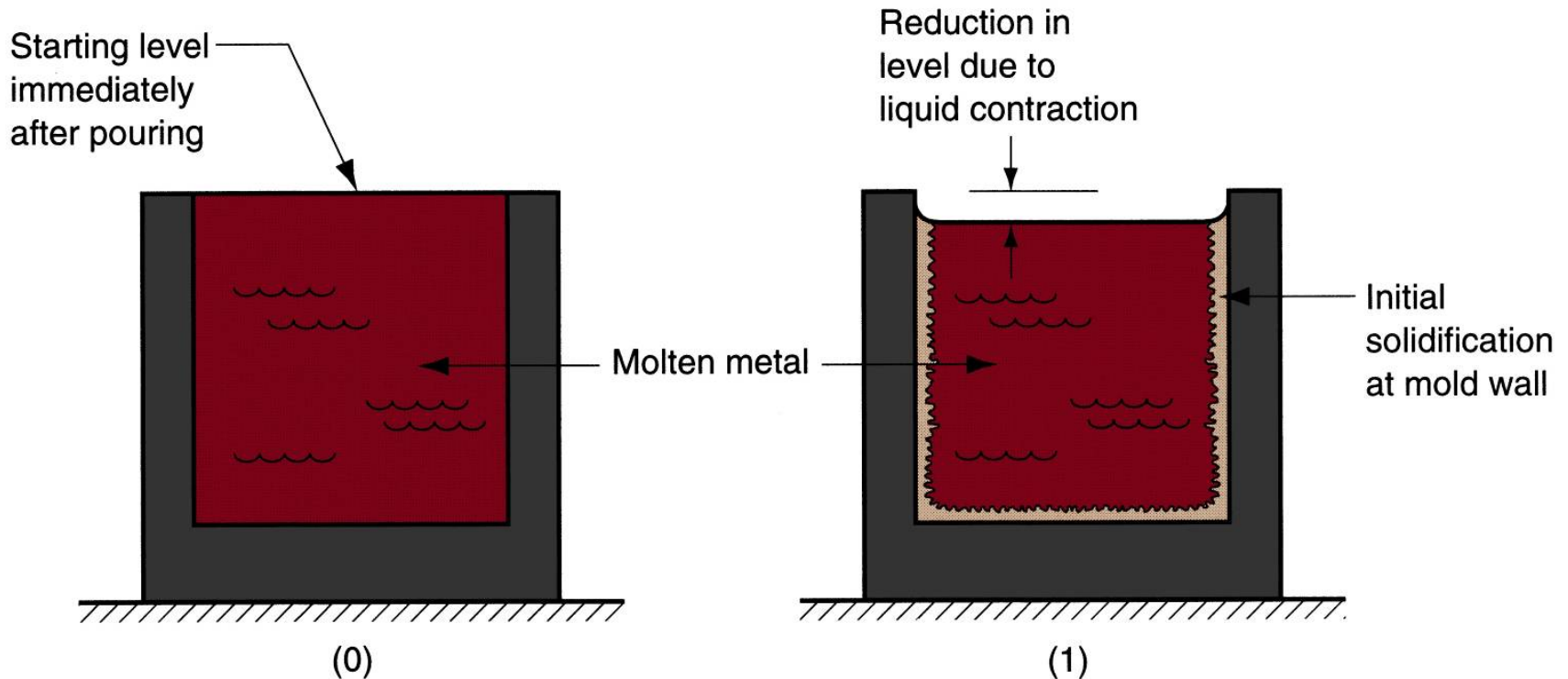
(b) Shrinkage

Crystallization is Controlled by Thermodynamics

- Volume is high as a hot liquid
- Volume **shrinks** as liquid is cooled
- At the melting point, T_m , the liquid crystallizes to the thermodynamically stable crystalline phase
- More compact (generally) crystalline phase has a smaller volume
- The crystal then shrinks as it is further cooled to room temperature
- Slope of the cooling curve for liquid and solid is the **thermal expansion coefficient, α**

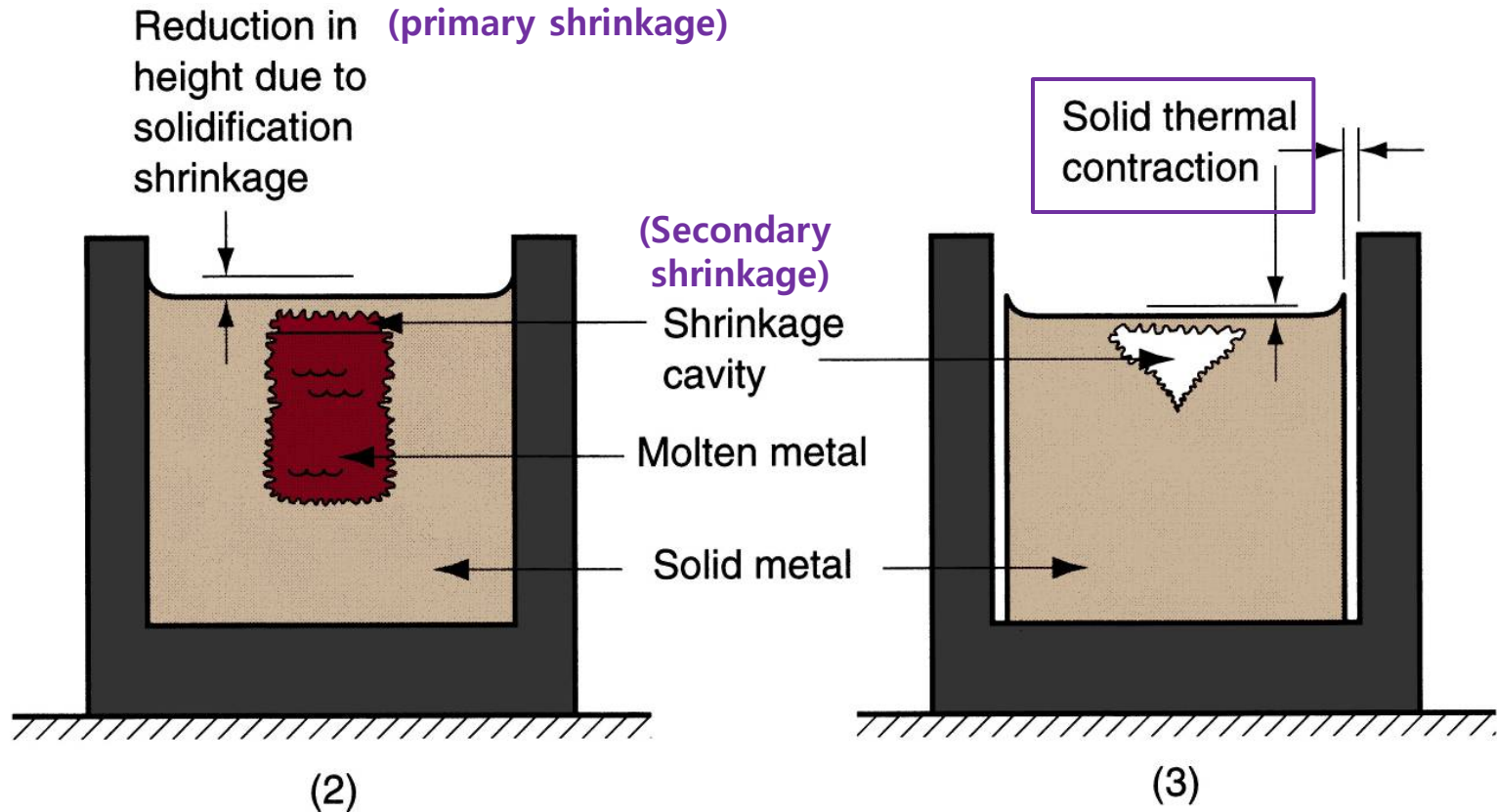


Shrinkage in Solidification and Cooling



- * Shrinkage of a cylindrical casting during solidification and cooling: (0) starting level of molten metal immediately after pouring; (1) reduction in level caused by liquid contraction during cooling (dimensional reductions are exaggerated for clarity).

Shrinkage in Solidification and Cooling



- * (2) reduction in height and formation of shrinkage cavity caused by solidification shrinkage; (3) further reduction in height and diameter due to thermal contraction during cooling of solid metal (dimensional reductions are exaggerated for clarity).

Shrinkage effect

* Formation of Voids during solidification

Central shrinkage:

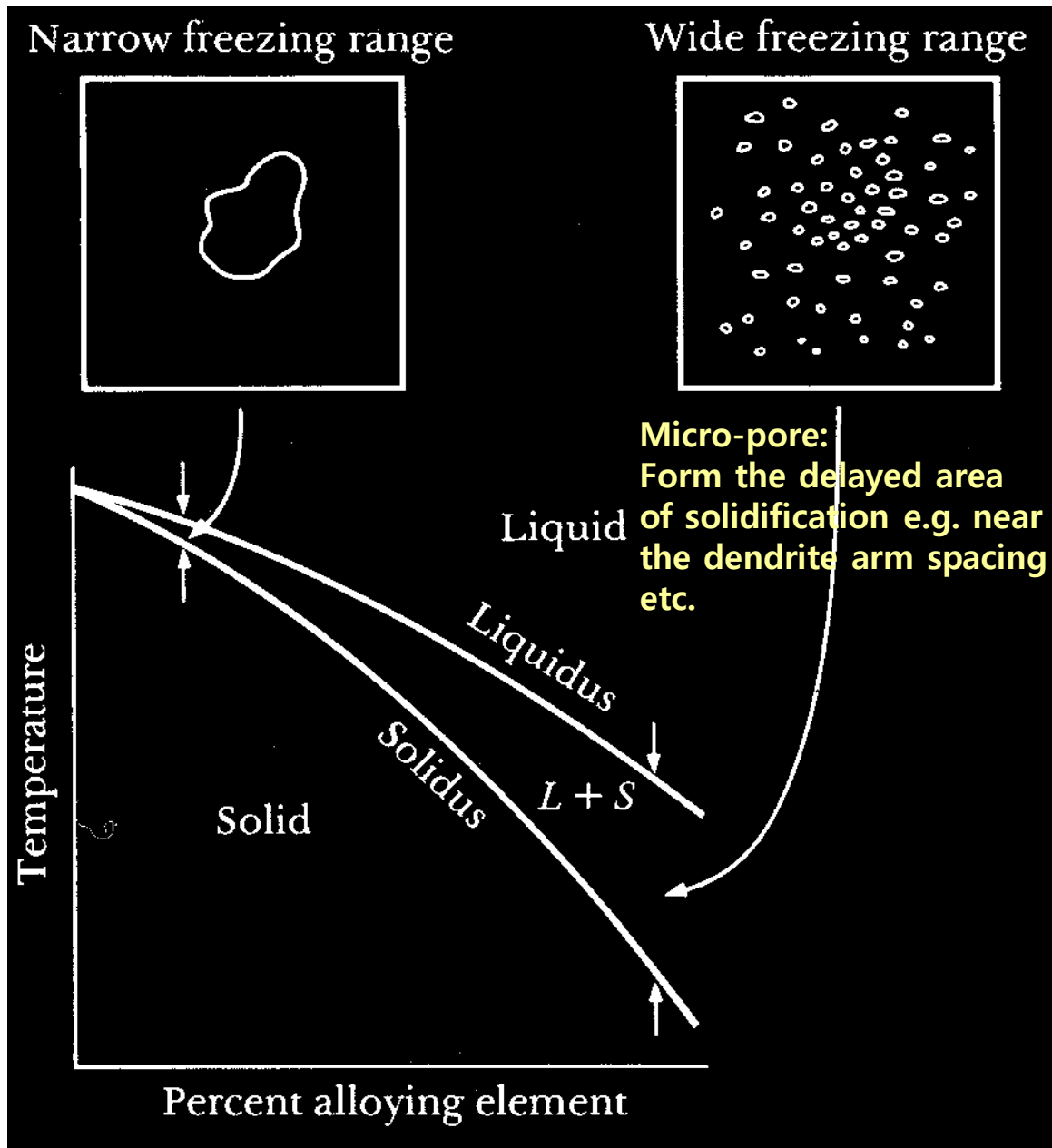
조성 변화가 크지 않은 주물의 응고 시 주로 응고수축, ΔV 에 의해 발생하는 주물 중심부에 발생

Dispersed Micro-Pore:

상당히 넓은 범위에 분산된 미소기공

외부수축 (몰드 주위) 및 1차수축공 (표면) 을 제외하면, 이러한 수축공 결함은 주로 기포 결함임

기포 내에는 철합금에서는 CO, 질소, 산소, 수소 등이, 동합금에서는 수소, 산소, 알루미늄 합금에서는 수소 등의 가스가 존재



Shrinkage in Solidification and Cooling

- Can amount to 5-10% by volume
- Gray cast iron expands upon solidification due to phase changes
- Need to design part and mold to take this amount into consideration

TABLE 5.1

Metal or alloy	Volumetric solidification contraction (%)	Metal or alloy	Volumetric solidification contraction (%)
Aluminum	6.6	70%Cu–30%Zn	4.5
Al–4.5%Cu	6.3	90%Cu–10%Al	4
Al–12%Si	3.8	Gray iron	Expansion to 2.5
Carbon steel	2.5–3	Magnesium	4.2
1% carbon steel	4	White iron	4–5.5
Copper	4.9	Zinc	6.5

Source: After R. A. Flinn.

* **Volumetric solidification expansion: H₂O (10%), Si (20%), Ge**

ex) Al-Si eutectic alloy (casting alloy) → volumetric solidification contraction of Al substitutes volumetric solidification expansion of Si.

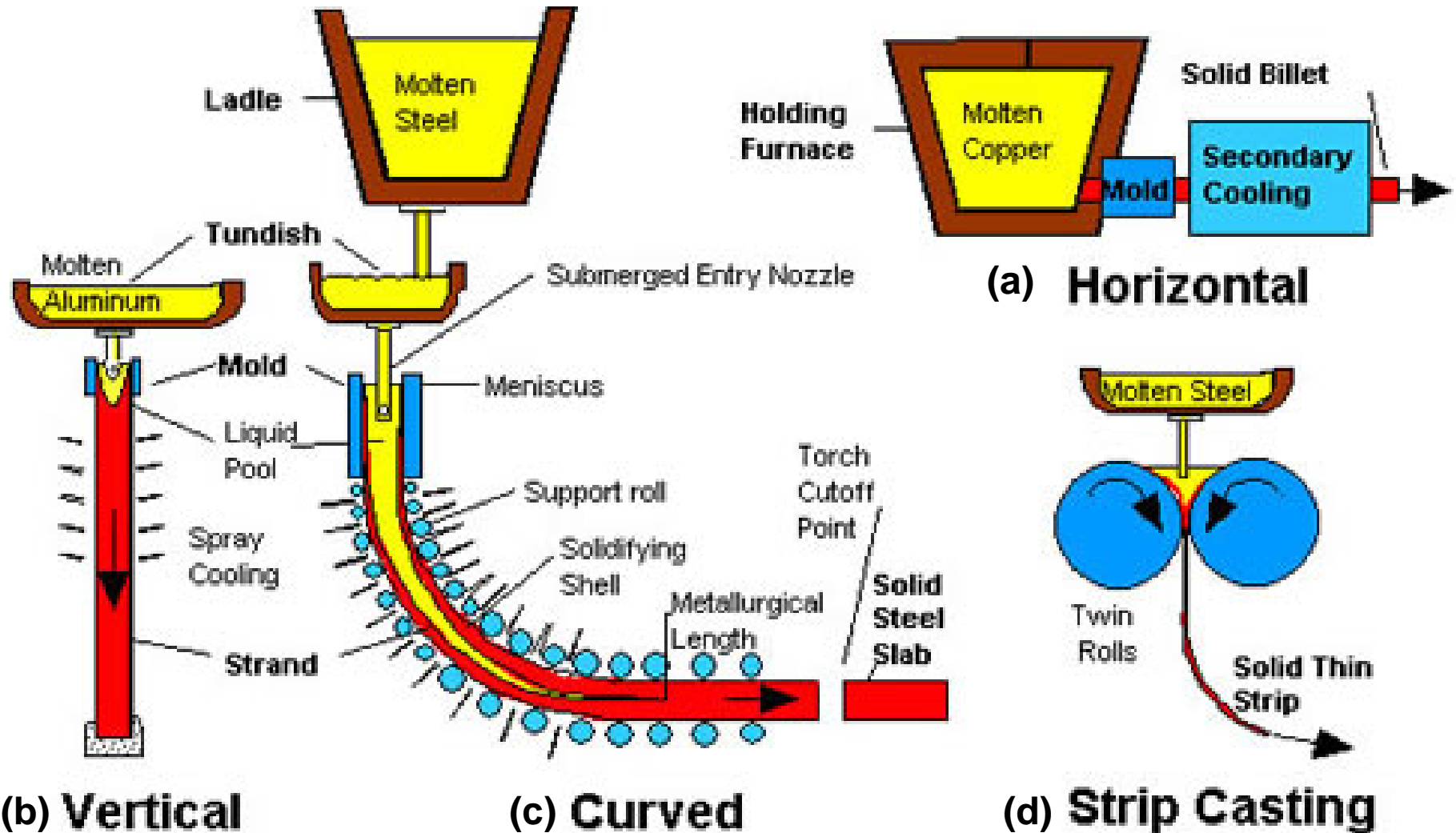
Cast Iron: Fe + Carbon (~ 4%) + Si (~2%)

→ precipitation of graphite during solidification reduces shrinkage.

Q: What is continuous casting?

4.4.3 continuous casting: a number of dynamic industrial process

The molten metal is poured continuously into a water-cooled mold from which the solidified metal is continuously withdrawn in plate or rod form. (solid-liquid interface)



“Dynamic process: importance of isotherm distribution”

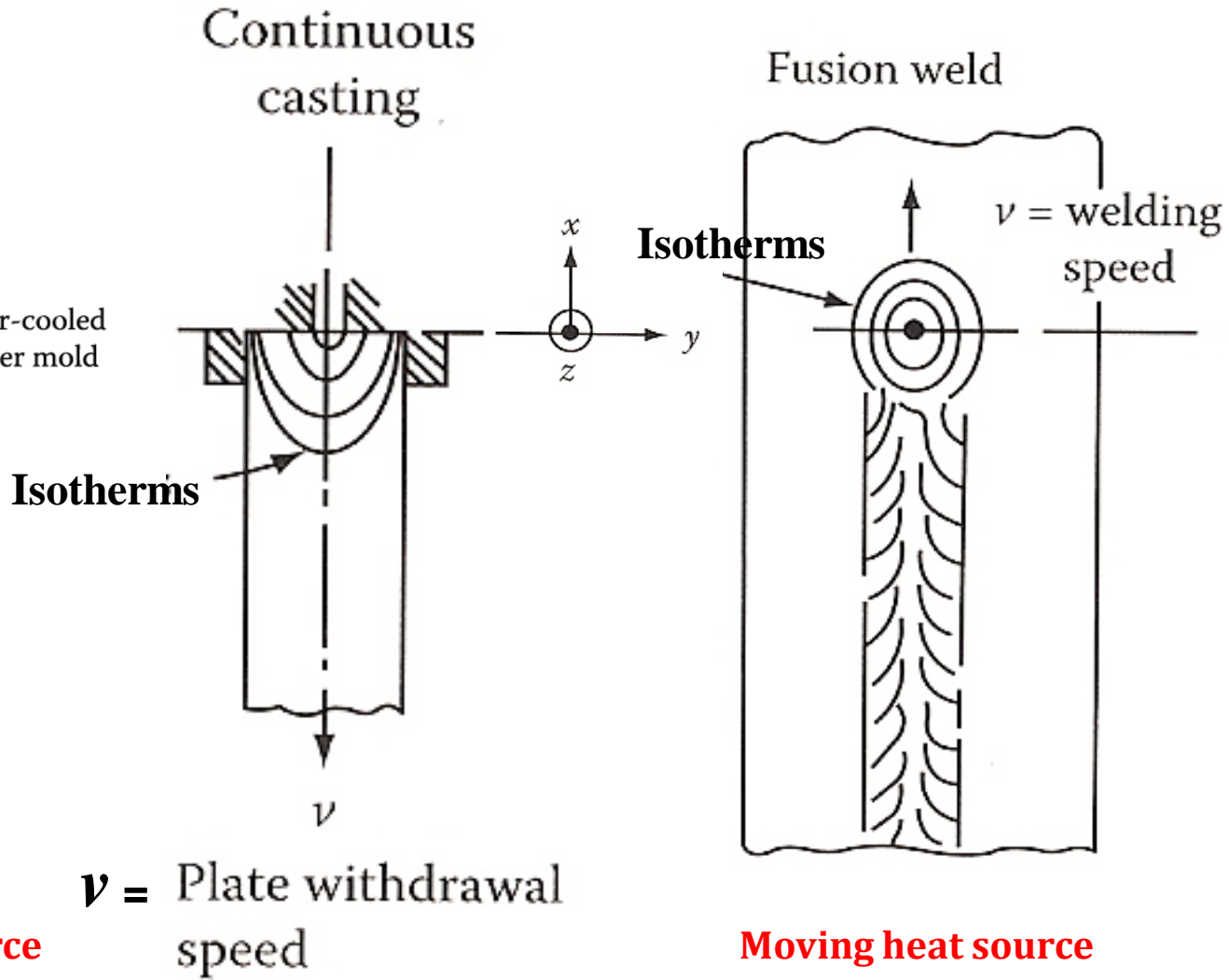
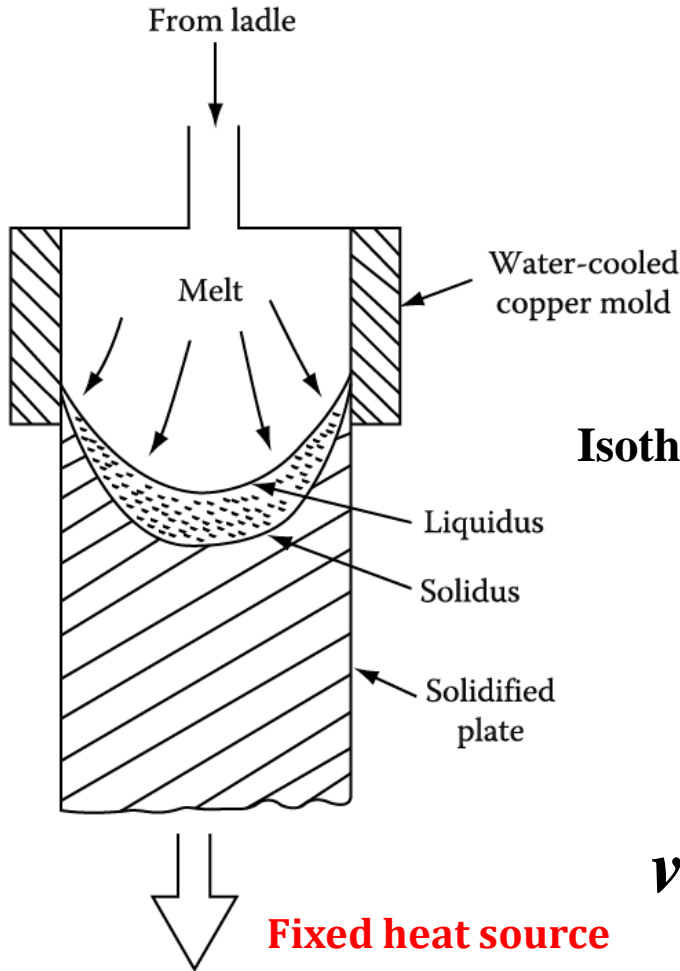


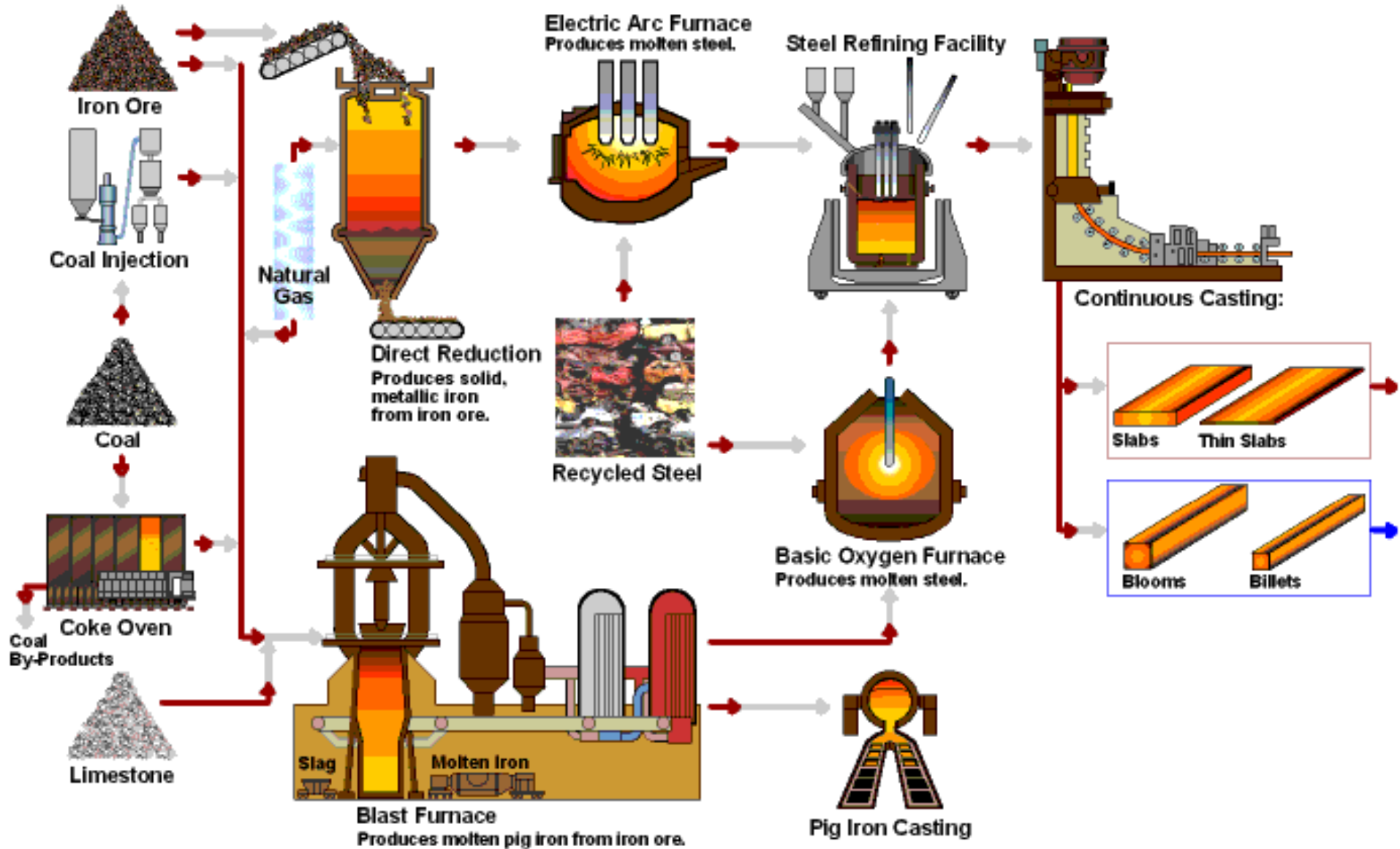
Fig. 4.44 Schematic illustration of a continuous casting process

Fig. 4.45 Illustrating the essential equivalence of isotherms about the heat sources in fusion welding and continuous casting

4.4.3 continuous casting



4.4.3 continuous casting



4.4.3 continuous casting

